IMPLEMENTATION OF REMOTE SENSING TECHNIQUE FOR MONITORING RIVER WATER QUALITY: A CASE STUDY ON DHALESHWARI RIVER IN SAVAR

CHOWDHURY MOHAMMAD TOUFIQ AMIN
(B.Sc in Civil Engineering)

A THESIS SUBMITTED FOR THE DEGREE OF MASTER OF SCIENCE IN CIVIL ENGINEERING

DEPARTMENT OF CIVIL ENGINEERING
MILITARY INSTITUTE OF SCIENCE AND TECHNOLOGY

December, 2019

DECLARATION

I hereby declare that this thesis is my original work and it has been written by me entirety. I have duly acknowledged all the sources of information which have been used in the thesis. This thesis has also not been submitted for any degree in any university previously.

_____

Chowdhury Mohammad Toufiq Amin

December, 2019

CERTIFICATION OF APPROVAL

We hereby recommend that the M.Sc Engg. Research work presented by Chowdhury Mohammad Toufiq Amin entitled "**Implementation of Remote Sensing Technique for Monitoring River Water Quality: A Case Study on Dhaleshwari River in Savar"** be accepted as fulfilling this part of the requirement for the degree of Master of Science in Civil Engineering.

BOARD OF EXAMINERS

Dr. Afzal Ahmed — Chairman
Professor — (Supervisor)
Department of Civil Engineering
Ahsanullah University of Science and Technology

Brig Gen Md Wahidul Islam SUP,ndc,psc — Member
Head — (Ex-officio)
Department of Civil Engineering
Military Institute of Science and Technology

Dr. Md. Tauhid Ur Rahman — Member
Professor
Department of Civil Engineering
Military Institute of Science and Technology

Dr. Md. Mafizur Rahman — Member
Professor
Department of Civil Engineering
Bangladesh University of Engineering and Technology

ABSTRACT

Monitoring river water quality is very important for a riverine country like Bangladesh. In the developed nations many agencies are involved in the continuous monitoring of the water bodies including rivers and lakes. In Bangladesh, only lab testing procedures are followed for assessing the water conditions. But this approach is both time-consuming and expensive. Moreover, it is not possible every time to collect water samples from any point and test immediately for the non-availability of laboratories. Remote sensing technique is a new technology for monitoring water quality which is very time efficient and also cost-effective. This study was undertaken by analyzing data from satellite images (Sentinel 2A) and geographical information systems (GIS) to find the relationship between water quality parameters, reflectance values and water indices of spectral images. The main purpose of this research was to develop a model for the physical and chemical parameters of the Dhaleshwari River in Savar. The water parameters used in this study are Acidity (pH), Total Dissolved Solids (TDS), Total Suspended Solids (TSS), Dissolved Oxygen (DO), Color and Turbidity. Samples from 10 points were collected and tested in the laboratory. At the same time, satellite images (Sentinel 2-A) of the sample collection date were downloaded and reflectance values were extracted from the satellite images. Finally, equations were developed incorporating the reflectance values and lab test values only. There are few water indices which are very useful in predicting the water bodies of an area. In the second part of the study, few important indices were calculated and regression equations were generated. Finally, equations with the highest regression values had been proposed to use in this study. A positive strong correlation between calculated water indices from satellite images and water parameters of the second day with 10 points helped to build some regression equations. These models could be used to predict these six water parameters at any point along the stream in Savar from the satellite image directly.

ACKNOWLEDGEMENT

All praise to Almighty Allah, the most beneficent and merciful who gave me enough courage and patience in this endeavor.

I would like to express my sincere gratitude to my advisor Prof. Afzal Ahmed for the continuous support of my M.Sc. study and related research, for his patience, motivation, and immense knowledge. His guidance helped me in all the time of research and writing of this thesis.

Next, I would like to thank Mr. Zahedul Islam of SPAARSO for assisting me with all his knowledge of remote sensing. It made the research more accurate. Special gratitude goes out to SAE Abul Kalam Azad of Environmental Engineering Lab for his support with lab testing.

I am grateful to my parents, my brother and my wife who have provided me with moral and emotional support in my life. I am also grateful to my other family members and friends who have supported me along the way.

Lastly, I want to thank my students Sakib Raihan, Raihanul Islam and Syful Islam for helping me in the data collection process.

Chowdhury Mohammad Toufiq Amin

Table of Content

List of Tables

List of Figures

Abbreviations and Notations

AWEI	Automated Water Extraction Index
BIWTA	Bangladesh Inland Water Transport Authority
BOD	Biochemical Oxygen Demand
CDOM	Colored Dissolved Organic Matter
CEGIS	Center for Environmental and Geographic Information Services
CETP	Central Effluent Treatment Plant
CZCS	Coastal Zone Color Scanner
DO	Dissolved Oxygen
DoE	Department of Environment
ECR	Environmental Conservation Rule
EQS	Environmental Quality Standard
GIS	Geographic Information System
GloVIS	Global Visualization Viewer
LISS	Linear Imaging and Self Scanning
MNDWI	Modification of Normalised Difference Water Index
MODIS	Moderate Resolution Imaging Spectro-radiometer
NDMI	Normalized Difference Moisture Index
NDWI	Normalized Difference Water Index
TDS	Total Dissolved Solids
TSM	Total Suspended Matter
TSS	Total Suspended Solids
USGS	U.S. Geological Survey
WiFS	Wide Field Sensor
WRI	Water Ratio Index

CHAPTER 1

INTRODUCTION

1.1 Background

The rivers surrounding Dhaka city namely Turag, Buriganga, Dhaleshwari, Balu, Shitalakhya and Tongi Khal are severe victims of environmental pollution due to the discharge of untreated effluents from industries, municipalities as well as other wastes. The relocation of tannery industries from Hazaribagh to Savar made the pollution scenario of the Dhaleshwari River more vulnerable than ever before. Our study area which includes a stretch of Dhaleshwari River flows through Savar Upazila located on the west of Dhaka City. The average depth of Dhaleshwari River is 122 feet (37 m) and the maximum depth is 265 feet (81 m) and the length is 160 kilometers (99 mi). Due to the continuous disposal of liquid and solid waste into the river, the water quality is degrading day by day. Fisheries and other aquatic lives are facing a severe threat. As different harmful chemicals and pollutants are mixing with river water, the local people cannot use it for their household purposes. Therefore, the water quality monitoring for this river is needed in order to raise awareness of the public by addressing the consequences of present and future threats of contamination.

Monitoring and assessing the quality of surface waters are critical for managing and improving its quality. In situ measurements and collection of water samples for subsequent laboratory, analyses are currently used to evaluate various water quality parameters. The method of in situ measurements of water quality characteristics is limited, especially with respect to spatial and temporal coverage because of the high cost of data collection as well as of laboratory analysis. Currently, advancement in remote sensing technology, image

analysis techniques and geographical information system provides significant support to monitor and predict water quality parameters for rivers, streams and other water bodies.

The five peripheral rivers of Dhaka city are the receivers of storm-water, municipal and industrial wastewater and sewage from the City (Paul and Haq, 2010). There are approximately 300 outfalls of domestic and industrial effluents that are discharged into the rivers without any treatment. The rivers are further polluted by indiscriminate throwing of household, clinical, pathological and commercial wastes and discharge of spent fuel and human excreta. In fact, the rivers have become a dumping ground of all kinds of solid, liquid and chemical waste of bank-side people (Rahman and Hadiuzzaman, 2005). The industrial units such as chemicals, fertilizers, pesticides, textile, oil, power station, ship repairing dock, cement and tannery are located in and around Dhaka City (DoE, 1993).

The worldwide systematic monitoring of environmental pollution by heavy metals began in the 1960s (Salomons, 1993). Pollution of the natural environment by heavy metals is a worldwide problem because these metals are indestructible and most of them have toxic effects on living organisms when they exceed a certain concentration (Nuremberg, 1984). Heavy metals are one of the serious pollutants in the natural environment due to their toxicity, persistence and bioaccumulation problems (Nouri et al., 2006). Heavy metals contamination in the river is one of the major quality issues in many fast-growing cities because the maintenance of water quality and sanitation infrastructure did not increase along with population and urbanization growth especially for the developing countries (Ahmed et al., 2010). Trace metals enter the river from a variety of sources; it can be either natural or anthropogenic (Bem et al., 2003). The main anthropogenic sources of heavy metal contamination are mining. Disposal of untreated and partially treated effluents contain toxic metals, as well as metal chelates from different industries (Hatje et al., 1998).

1.2 Objectives

The objective of this research is to develop suitable regression models for water quality monitoring of Dhaleshwari River incorporating field data with both the reflectance values and water indices extracted from digital images. The specific objectives of this research are:

1. To assess river water quality by measuring physical and chemical water quality parameters through laboratory experiments of water samples collected from different points on the Dhaleshwari river.
2. To assess the spatio-temporal pattern of water quality parameters of Dhaleshwari River using remote sensing techniques through extracting various reflectance values and subsequently measuring the water indices from digital images.
3. To develop two types of regression model, incorporating the measured values from the lab tests with satellite images reflectance values and subsequently with important water indices.

1.3 Study Area

Dhaleshwari River is an important resource of water for Savar area for its many uses. It is a distributary of the Jamuna River that takes off in the northwestern part of Tangail district. It is a meandering river having two branches. The main stream flows north of Manikganj and joins the other branch, the Kaliganga, south of Manikganj. The Kaliganga again joins with the Dhaleshwari. It meets the Shitalakshya river near Narayanganj and flows south to meet the Meghna near Shaitnol and then loses its separate identity.

For this research, only the newly built tannery portion of Dhaleshwari river spreading through Savar union was chosen. It supports the habitat for aquatic ecosystem including a wide variety of fishes as well as the riparian vegetation. The insecticides, pesticides and fertilizers used in the surrounding cultivated lands are frequently polluting the river by washing out through surface runoff mostly during the rainy season. People nearby the river

use its water for washing their clothes, bathing, washing their cattle etc. These anthropogenic activities may degrade the quality of the river water. Savar is known to be a very important industrial zone. A lot of industries have been built here in this area. Also, the tannery industry in Hazaribagh has been relocated to Savar, on the bank of Dhaleshwari river. Though this relocation was intended to protect Buriganga river from the pollution of tannery effluent, the untreated toxic effluents are now seriously polluting the Dhaleshwari river, putting its existence and biodiversity at stake. So, this area was chosen as this area is more in danger of pollution than other areas. The following figure 1.1 shows the study area and its surroundings and highlighting the boundary of tannery industry at the bank of the river. Water sample collection locations are indicated with point markers in this figure and their coordinates are presented in table 1.1.

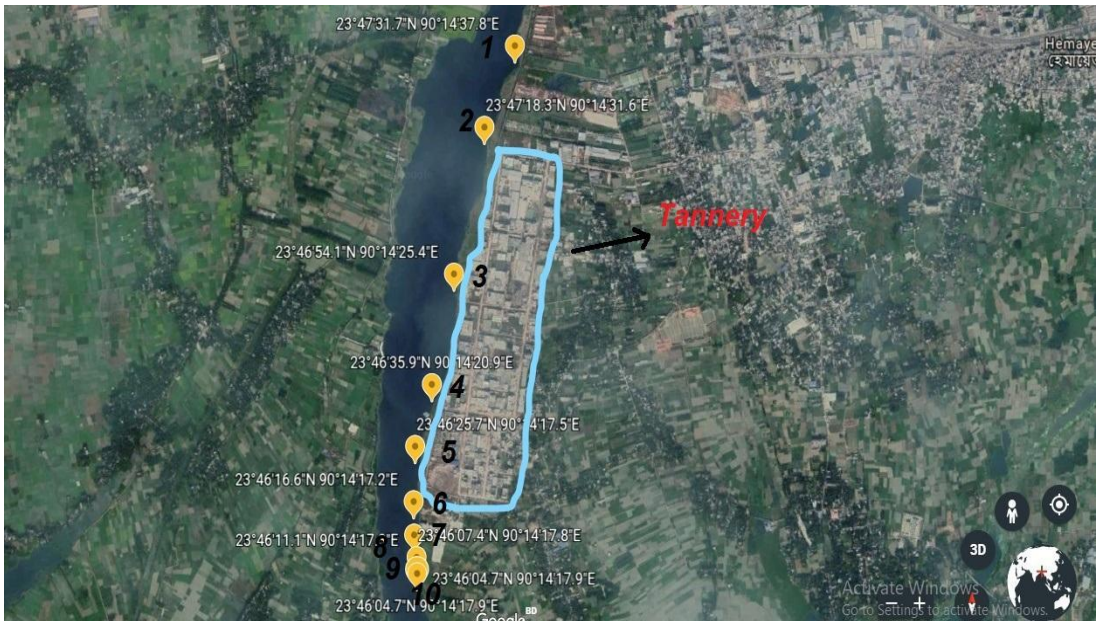

Fig 1.1: Sample locations around Savar tannery estate

Table 1.1: Coordinates of the selected locations

Point	Lat/Long
1	N 23° 47' 31.7", E 090° 14' 37.8"
2	N 23° 47' 18.3”, E 090° 14' 31.6"
3	N 23° 46' 54.1", E 090° 14' 25.4"
4	N 23° 46' 35.9", E 090° 14' 20.9"

5	N 23° 46' 34", E 090° 14' 19.7"
6	N 23° 46' 25.7", E 090° 14' 17.5"
7	N 23° 46' 16.6", E 090° 14' 17.2"
8	N 23° 46' 11.1", E 090° 14' 17.3"
9	N 23° 46' 07.4", E 090° 14' 17.8"
10	N 23° 46' 04.7", E 090° 14' 17.9"

1.4 Organization of Thesis

Chapter 1 describes the background and objectives of the study. Also, description of the study area is included in this chapter.

Chapter 2 illustrates the previous significant studies where remote sensing techniques were used. Studies conducted by Bangladeshi professionals are mentioned here. Important water quality parameters and their significance in maintaining water body are also described. This chapter also gives the basic idea of remote sensing and important water indices respectively.

In **Chapter 3** detail research methodology has been described. Firstly, the field measurement has been described. Sample collection procedure and standard lab testing procedure for every water parameter is described first. Subsequently, satellite image downloading and image processing have been shown step by step here. Finally, a summary of the equation generation procedure is mentioned.

Chapter 4 mainly shows all the outputs from every steps of methodology from field data to regression equations. It includes the lab test results, reflectance values, water indices calculation and finally the generated equations.

Final conclusions of the study are represented in a summary form in chapter 5. There were some limitations while conducting this study, which are discussed in this chapter. Finally, some recommendations have been proposed for further study as a continuation of this research work.

CHAPTER 2

LITERATURE REVIEW

2.1 Introduction

Water quality monitoring is very much needed to control the pollution especially for river around Dhaka City. Encroachment of the river area, continuous dumping to river and unplanned industrial growth around river has damaged the overall condition of river ecosystem. In the developed countries, some groups are always active in the monitoring the river water quality. They provide the data to the national level organization regularly to appraise the authority about the scenario of the water bodies. In our country, there are no such systems of monitoring. There are many techniques of water quality monitoring for river water. Laboratory testing is the most popular method of testing the water. But there is not enough number of Environment Laboratory in our country. There are smaller scale instruments which can be used for in-situ measurement of water. But the in situ measurement is very time consuming and also not cost effective. Remote Sensing and Geographic Information System (GIS) are very effective tools for monitoring of water quality and its pollution over the Oceanic areas, Lakes, Reservoirs and Rivers. Now a days Hyper-spectral and Multispectral Satellite imageries play a vital role in the determination and Monitoring of water quality. Satellite imageries such as MODIS, Sentinel, Hyperion, Landsat, Linear Imaging and Self Scanning (LISS) and Wide Field Sensor (WiFS) ProbaChris have been used successfully in monitoring of various water quality parameters like TSS, TDS, Turbidity, Chlorophyll, Total Hardness, Electrical Conductivity content, color, temperature, Dissolved Oxygen etc. The Remote Sensing techniques have been used in sustainable management of water resources, which include runoff and hydrological modeling, flood management, watershed management, drought management and management of Irrigation Command Areas.

2.2 Water Quality Standards

River water has various purposes mainly domestic and drinking purposes. So the maintenance of quality is a very much important factor. The lives of the people living near the river and the aquatic plants are directly dependent on it. A total of 6 parameters have been considered in our study.

2.3 Water Quality Parameters

The health of a river depends on the quality of its water, which is influenced by the presence of pollutants. The quality of water is generally assessed by a range of parameters, which express physical, chemical and biological composition of water (Meybeck and Helmer 1992). This research deals with some specific water quality parameters of the Dhaleshwari River, which include: pH, Color, Dissolved Oxygen (DO), Total Dissolved Solid (TDS), Total Suspended Solid (TSS) and Turbidity.

2.4 Basic of Remote Sensing

Remote Sensing is the art and science of acquiring information about the earth surface without having any physical contact with it. This is done by sensing and recording of reflected and emitted energy. Remote Sensing involves an interaction between the incoming radiation and interest of target. This is done by using imaging and non-imaging system; however, the following steps are involved in the process:

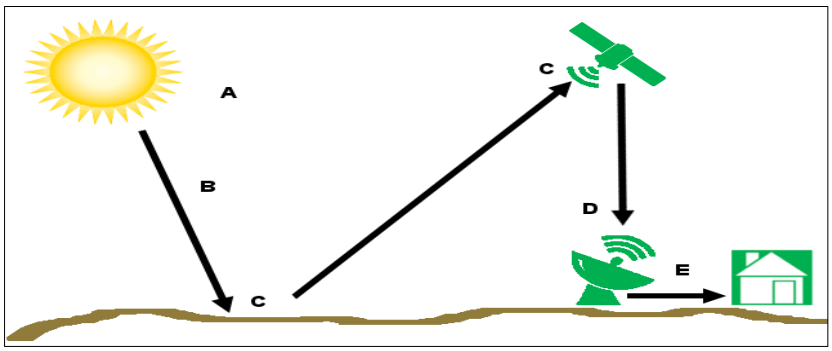

Fig 2.1: Basic overview of remote sensing

a. Energy Sources:

The first and most important requirement for a remote sensing system is an ideal energy source or illumination which provides electromagnetic radiation to the target of interest.

b. Atmosphere and Radiation:

As the energy traveling from its source to Earth surface, it will come in contact with atmosphere when it passes through. This is also happening when the energy from target reflected back to sensor.

c. Interaction with the Target and Recording of the Reflected Energy:

Once the energy is passed through the atmosphere, it interacts with the target object and depending upon the physical and chemical properties of the target, the energy is reflected or emitted back. The sensor collects and records the electromagnetic radiation.

d. Transmission and Ground Level Processing:

After the energy is sensed, it has to be transmitted in the form of electronic signals to the ground stations for processing and generating the output as image.

e. Interpretation, Analysis and Application.

The processed image is interpreted visually and digitally using various interpretation Techniques to extract the information.

2.5 Remote Sensing Indices for Water Quality Monitoring

Modification of Normalized Difference Water Index (MNDWI)

The modified NDWI (MNDWI) can enhance open water features while efficiently suppressing and even removing built-up land noise as well as vegetation and soil noise. The enhanced water information using the NDWI is often mixed with built-up land noise and the area of extracted water is thus overestimated.

Three results are expected from using the MNDWI model; (1) greater positive values for water as water absorbs more MIR light than NIR light; (2) negative values for built-up land

because of its higher reflectance in the MIR light than in NIR light and (3) soil and vegetation will still have negative values (Xu, 2006).

Normalized Difference Water Index (NDWI)

The NDWI index is most appropriate for water body mapping. The water body has strong absorbability and low radiation in the range from visible to infrared wavelengths. The index uses the green and Near Infra-red bands of remote sensing images based on this phenomenon. The NDWI can enhance the water information effectively in most cases. It is sensitive to built-up land and often results in over-estimated water bodies. It is used to monitor changes related to water content in water bodies, using green and NIR wavelengths, defined by McFeeters (1996).

Normalized Difference Moisture Index (NDMI)

This index contrasts the near-infrared (NIR) band 4, which is sensitive to the reflectance of leaf chlorophyll content to the mid-infrared (MIR) band 5, which is sensitive to the absorbance of leaf moisture.

2.6 Few Important Water Index

After doing the image analysis, the reflectance values are used to determine water indices. Few important water indices and their formulas are given below-

Table 2.1: Water indices and their formulas

Index	Formula
Normalized Difference Water Index (NDWI)	$NDWI = \frac{GREEN - NIR}{GREEN + NIR}$
Modification of Normalized Difference Water Index (MNDWI)	$MNDWI = \frac{GREEN - SWIR2}{GREEN + SWIR2}$
Normalized Difference Moisture Index (NDMI)	$NDMI = \frac{RED - NIR}{RED + NIR}$
Automated Water Extraction Index (AWEI)	$AWEI = 4 * (GREEN - SWIR2) - (0.25 * NIR + 2.75 * SWIR1)$
Water Ratio Index (WRI)	$WRI = \frac{GREEN + RED}{NIR + SWIR2}$

2.7 Sentinel-2A

Many suitable sensors are available for estimating water quality. Sensors are compared and selected based on their spectral, spatial and temporal resolution. A high spectral resolution is desired to differentiate substances based on their reflectance spectrum. There are few satellites which have suitable and high spectral resolution sensor. Sentinel-2A is an Earth monitoring satellite developed as a part of the Copernicus programme by Airbus Defence and Space (ADS) for the European Space Agency (ESA). The Copernicus programme aims to establish European capacity for earth observation. It was formerly known as the European Global Monitoring for Environment and Security (GMES) programme and is funded jointly by the European Commission and the ESA. Sentinel-2A satellite was launched from Plesetsk Cosmodrome in June 2015. It was placed at a 786km altitude in the Sun synchronous orbit. It will image the Earth's land masses and deliver operational applications in the field of agriculture, forestry, land cover and cartography. It will also offer support for humanitarian relief work and extraction of geophysical variables from vegetation. The Sentinel-2A is the first of the twin satellite Sentinel-2 constellation. (Aerospace-technology)

The span of 13 spectral bands, from the visible and the near-infrared to the shortwave infrared at different spatial resolutions ranging from 10 to 60 meters on the ground, takes global land monitoring to an unprecedented level. The four bands at 10 meter resolution ensure continuity with missions such as SPOT-5 or Landsat-8 and address user requirements, in particular, for basic land-cover classification. The six bands at 20 meter resolution satisfy requirements for enhanced land-cover classification and for the retrieval of geophysical parameters. Bands at 60 meter are dedicated mainly to atmospheric corrections and cirrus-cloud screening. Sentinel-2A satellite is the first civil optical Earth

observation mission of its kind to include three bands in the ‘red edge', which provide key information on the vegetation state.

2.8 Previous Studies

The development of remote sensing techniques during 1970s and 1980s in particular the launch of space instruments dedicated to the observation of earth’s environments such as Landsat MSS and, later the AVHRR series of instruments, stimulated research and promoted new applications. Progress in the monitoring and characterization of plant canopies and ecosystems on the basis of space observations has been achieved in various directions. One of the remote sensing’s applications is water quality which has been studied since the 1980s with different sensors in almost every inland water, Here are several main recent previous studies which have considered the issue of this study earlier by using the remote sensing and GIS techniques for the water quality parameters over the past few years.

X. Xiao et al (2015) used multispectral remote sensing data for the rapid water quality assessment of Han River in China. The research was basically conducted in two phases. In the first phase, water quality index model was established and in the second phase water quality was assessed with the model. Images from two domestic satellites were used to establish the model.

Shareef M A. et al (2014) used a new method for estimating water quality parameters. Traditional method of remote sensing involves relying on spectral response or scattering reflected from water. Here a new theory of texture analysis has been introduced. To assess the contamination of water, empirical statistical models have been developed. Six texture parameters were estimated in this study.

Papoutsa C. et al (2017) did a Case Study of Asprokremmos Dam in Cyprus to monitor water quality using remote sensing. Their study area Asprokremmos Dam is built at an altitude of about 100 meters above sea level and is located 16 kilometers east of the city of

Paphos. Eleven (11) Landsat TM/ETM+ satellite images were used in order to investigate how satellite remotely sensed data can become a valuable tool to monitor and assess the temporal variations of water quality in Asprokremmos Dam. All the images were pre-processed including geometric and atmospheric correction steps. The Landsat TM sensor's temporal coverage, spatial resolution, and data accessibility make it especially useful for monitoring inland water bodies (Kloiber et al. 2002; Zhou et al. 2006).

The Landsat TM sensor is currently used to measure TSS and chlorophyll-a found in surface water. The majority of researchers have concluded that the concentration of total suspended solids (Schiebe et al. 1992; Dekker and Peters 2002; Wang et al. 2006; Zhou et al. 2006) and chlorophyll-a (Ritchie et al. 1990; Ekstrand 1998; Schiebe et al. 1992; Giardino et al. 2001, Han and Jordan 2005) can be mapped for large water bodies using currently available sensor data. Landsat TM bands 1-4 are within the spectral range (400-900 nm) able to penetrate water and thus capable of providing useful water quality information (Dekker and Peters 1993).

Suspended sediments in surface water increase the spectral radiance of the visible light and near-infrared portions of the electromagnetic spectrum (Ritchie et al. 1976). Results of a study estimating total suspended solids from remotely sensed water reflectance conducted by Novo et al. (1991) proved that there is a significant and constant correlation between spectral reflectance from 450-900 μm and TSS. Many studies have successfully estimated water quality concentrations by implementing regression models with single TM bands and band ratios as independent variables (Ritchie et al. 1990, Lathrop 1992, Dekker and Peters 1993, Wang et al. 2006). Different band and band ratios have been found to successfully estimate a single water quality parameter (Wang et al. 2006). The regression values of the equations were very high (0.7-0.8)

Several other studies have been conducted implementing remote sensing technologies to estimate total suspended solids in surface waters. Lathrop conducted an investigation on the relationship between water quality and spectral reflectance and concluded band ratios TM2/TM1 and TM3/TM1 had the strongest relationship to total suspended solids (1992). In a study mapping, total suspended matter (TSM) in Lake Taihu, China, Zhou et al. (2006) found TM3 was the most significant predictor of TSM during different seasons regardless of algae concentration. Total suspended matter is another term for total suspended solids. The average of bands TM2 and TM3 has also been used to establish the relationship between total suspended solids and spectral radiance (Dekker et al. 2002).

According to Dekker and Peters (1993), Band 4 reflectance is "the product of rapidly increasing water absorption and probably suspended matter reflection". Ekstrand (1998) concluded that TM band 4 could be implemented to successfully estimate surface water chlorophyll-a concentrations in coastal waters. Band ratios have been proven especially useful for establishing the relationship between chlorophyll-concentrations due to its characteristic scattering and absorption properties (Dekker et al. 1991). Han and Jordan (2005) implemented the band ratio TM1/TM3 to estimate and map chlorophyll-a concentrations in Pensacola Bay, Florida. In a similar study, Wang et al. (2006) found the band ratio TM3/TM2 best explained the variance of chlorophyll-a concentration in Reelfoot Lake, Tennessee. Band ratio TM1/TM2 has also been successfully implemented to establish an empirical relationship used to map chlorophyll-a concentration (Dwivedi and Narain 1987).

Ming et al. (1996) have established an integrated water quality models with GIS techniques in central Taiwan. This model is developed as a water quality monitoring system data which obtained from SPOT data to get the distribution of chlorophyll-a, Secchi depth (SD) and phosphorus using ERDAS IMAGINE software. Moreover, an approach simulation system

is used to estimate the complexity of water quality. The model is based on the band ratio regression to show the water quality conditions for remote sensing monitoring. Consistent with the theoretical basis, red-band infrared band correlation matrix shows the highest rate of chlorophyll correlation and green / red (XS1 / XS2) ratio have a significant correlation with Secchi depth and phosphorus concentrations. A natural logarithmic regression model is also developed for chlorophyll-a, the Secchi depth (SD) and phosphate (PO4) and the results of the regression model shows a statistically significant (R2 = 0.95, P = 0.005) between the band ratios with chlorophyll-a and Secchi depth with a lower correlation (R2= 0.827, P = 0.032) for the phosphorus variable.

Hellwegera et al. (2004) have investigated utility of satellite imagery for water quality studies in New York Harbour. Ground data from a routine sampling program (New York Harbour Water Quality Survey) are compared to imagery from the Landsat Thematic Mapper (TM) and Terra Moderate Resolution Imaging Spectroradiometer (MODIS) sensors. Using a time-averaged spatial analysis, it is shown that turbidity as determined from Secchi depth correlates with Landsat TM red reflectance in regions affected by the Hudson River sediments (N=21, R2=0.85). Based on this correlation, the estuarine turbidity maximum of the Hudson River is mapped. Landsat TM red reflectance is also used to identify and map plumes of increased turbidity caused by rainfall runoff and/or Spring tide resuspension in Newark Bay. Chlorophyll-a concentration correlates with the ratio of Landsat TM green to red reflectance in the eutrophic East River and Long Island Sound (N=16, R2=0.78). Terra MODIS estimates of chlorophyll-a show no correlation with ground observations in New York Harbour.

Mustafa T. et al. (2017) did a research to develop a model for the physical and chemical parameters of Gharraf stream in Iraq. This study was undertaken by analyzing data from satellite image (Landsat-8 OLI) and geographical information system (GIS) to find the

relationship between water parameters and water indices of spectral images. The main purpose of this research was determination of Acidity (PH), Total Dissolved Solids (T.D.S), Alkalinity(ALK), Electrical Conductivity (E.C), Calcium(Ca), Chloride (CL), Sodium (Na), Sulfate (SO4), Potassium (k), Total suspended solid (T.S.S), Total Hardness (TH). A total of 17 points were selected for sampling of water and simultaneously Landsat images were collected for the sampling dates. Then different water indices were measured and were treated in SPSS software to find out the regression equations. The regression values were in the range of 0.7-0.9.

A research done by Jaelani & Limehuwey titled as "Estimation of TSS and Chl-a Concentration from Landsat 8-OLI: The Effect of Atmosphere and Retrieval Algorithm" describes a specific method of using remote sensing in water quality measurement. In this research, the accuracy of the atmospherically corrected product of USGS as well as the developed algorithms for estimating Chl-a concentration using Landsat 8-OLI data were evaluated. Landsat 8-OLI data at path/row of 117/65 were collected at concurrent field campaign time. These data collected on April 22, 2015 and October 15, 2015. Since the atmospheric correction algorithm to convert remote sensing reflectance from Top of Atmospheric (TOA, recorded by sensor) to Bottom of Atmosphere (BOA, surface reflectance) is difficult for Landsat data, the Surface Reflectance (SR) which processed by USGS was used directly. The surface reflectance data was atmospheric corrected data using internal algorithm (for Landsat 8) and based on 6S algorithm for prior Landsat 8 for 7 bands.

Hua et al. (2004) have explored the potential of Tampa Bay, FL for using MODIS medium-resolution bands (250- and 500-m data at 469-, 555-, and 645nm) for estuarine monitoring. Field surveys during 21–22 October 2003 has shown that Tampa Bay has a quality of waters, for the salinity range of 24–32 psu; chlorophyll concentration (11 to 23 mg m3),

coloured dissolved organic matter (CDOM) absorption coefficient at 400 nm (0.9 to 2.5 m1), and total suspended sediment concentration (2 to 11 mg L-1). CDOM is the only constituent that showed a linear, inverse relationship with surface salinity, although the slope of the relationship changed with location within the bay. The MODIS medium resolution bands, although designed for land use, are 4–5 times more sensitive than Landsat-7/ETM+ data and are comparable to or higher than those of Coastal Zone Color Scanner (CZCS). Several approaches are taken into account to derive synoptic maps of water constituents from concurrent MODIS medium-resolution data. They have found that application of various atmospheric-correction algorithms yielded no significant differences, due primarily to uncertainties in the sensor radiometric calibration and other sensor artefacts. However, where each scene could be ground trothed, simple regressions between in situ observations of constituents and at-sensor radiances provided reasonable synoptic maps. They have addressed the need for improvements of sensor calibration/characterization, atmospheric correction and bio-optical algorithms to make operational and quantitative use of these medium-resolution bands.

Akbar. et al. (2014) have developed, evaluated and applied the remote sensing based models for Canadian Water Quality Index (CWQI) and turbidity for the Bow River of Alberta. They have considered 31 scenes of Landsat-5 TM satellite data to establish the relationship between the planetary reflectance and the monthly ground measured data for the period of 5 years (2006 - 2010). The four spectral bands (blue, green, red, and near infrared) are used to obtain the most suitable models from 26 different band combinations. The best-fit models are validated with ground measured data and found that 72% of the data showed 100% matching for the CWQI model and 83% of the data for the turbidity model. The Landsat-5 TM based CWQI and turbidity models are applied on all the scenes to obtain five CWQI classes (excellent, good, fair, marginal and poor), and six classes of

turbidity (i.e. 0–10 NTU, 10–20 NTU, 20–30 NTU, 30–40 NTU, 40– 50 NTU, >50 NTU). The variation of river water quality in different years of interest is associated with the climatic changes. The most deteriorated water quality noted in two natural sub-regions included mixed grass and dry mixed grass, which could be related to irrigation-based farming.

A statistical analysis was performed to establish the relationship between water quality parameters obtained through satellite and those measured on the ground. Spearman's correlation test was performed to define the rate of association between two variables, to find out whether it is a positive or negative linear relationship (Kibena et al., 2014). The SPSS software was used to calculate the spearman's correlation rho (r). A critical value was determined for a 95 % confidence interval from the sample size, n, and the r (Faul et al., 2009). Ahsan Azhar Shopan et al (2015) used remote sensing techniques for the assessment of water quality parameters in the Ganges Delta. Temporal changes of water quality during 1989-2009 were assessed using remote sensing techniques. The study analyzed 3 landsat scenes of the study area acquired in 1989, 2000 and 2009. A total of 5 water indices were estimated in this study (Turbidity, Chlorophyll-a, SDD, Total Suspended Material and Colored Dissolved Organic Matter.

Hae-Cheol Kim et al (2017) used remote sensing techniques to find out seasonal trend with spatial heterogeneity. The study was done on the Yellow sea. A total of 10 areas along the western coast of the Korean Peninsula are investigated with respect to remotely sensed water quality indicators derived from NASA MODIS abroad of the satellite aqua. A strong six month long phase lag was found between chlorophyll-a and total suspended solid owing to their inversed seasonality, which could be explained by different dynamics and environmental settings. This study revealed the potential and applicability of satellite products in coastal management. It was found that remote sensing would be a promising

tool in resolving orthogonality of large spatio-temporal scale variabilities when combined with proper time series analysis.

M. Chawira et al (2013) used remote sensing for water quality monitoring in two of the most polluted inland water bodies (Lakes Chivero and Manyame) of Zimbabwe. Results indicate that remote sensing measurements are comparable with in situ measurements. A strong positive correlation between measured and modeled chl_a concentrations was obtained. Relationships between optically active water constituents were assessed. It was found that remote sensing data allows simultaneous retrieval of different water quality parameters as well as providing near real time and space results that can be used by water managers and policy makers to monitor water bodies.

Another study was conducted by Masocha M. et al (2017) where remote sensing was used to assess the surface water quality in relation to catchment condition in Zimbabwe. Normalized Difference Vegetation Index (NDVI) was used to assess how catchment condition varies within and across river catchments in Zimbabwe. In this study, remotely sensed Normalised Difference Vegetation Index (NDVI) was used to assess how catchment condition varies within and across river catchments in Zimbabwe. The results showed a consistent negative curvilinear relationship between Landsat 8 derived NDVI and TSS measured across the catchments under study. Our results suggest that NDVI derived from free and readily available multispectral Landsat series data (Landsat 8) is a potential valuable tool for the rapid assessment of physical water quality. Overall, the finding of this study revealed the usefulness of readily available satellite data for near-real time monitoring of the physical water quality at river catchment scale.

Rostom N G. et al (2016) evaluated water quality of Mariut Lake using hyperspectral remote sensing technique. This research included assessing of water contamination by heavy metal in Mariut lake using laboratory analysis and developing a predictive model for

water pollution based on spectral characteristics. High significant correlation (0.27 to 0.97) was found to predict heavy metal concentration. In some research works, statistical analysis has also been included. Narayan C Viswanath (2015) performed various statistical analysis of water quality for various watersheds in Kerala, India. Multivariate statistical analysis of groundwater quality was done for a total of 30 sampling points. 11 water parameters were analyzed by statistical analysis.

Rwatnakar et al (2017) developed a methodology for real-time water quality measurement in a river at 30 m spatial and 1 day temporal scales using satellite remote sensing technique to support daily water quality monitoring usually done at gauges. Considering the limited spatio-temporal resolutions of all the current satellite products, this study integrates the corrected band-specific Landsat and Moderate-resolution Imaging Spectroradiometer (MODIS) surface reflectance values, identified by a physically-based approach, with the observed pollutant concentrations. Linear and nonlinear regression analysis was carried out for these combinations using the SPSS software to get the best (significant) correlated relations. This formulation is applied and tested in the Brahmani River located in eastern India's Odisha state for its real-time application; and water quality mapping is carried out for a typical river reach of the Brahmani River.

Aminul S M. et al (2018) did analyze on physicochemical parameters, anions and major heavy metals of the river. The study was conducted on 3 different locations of the Dhaleshwari river from March to May 2016. The physicochemical parameters included color, odor, temperature, pH, DO, BOD, EC, TDS; anions included F^- , Cl^- , Br^- , NO_3^- , NO_2^- , SO_4^{2-} and PO_4^{3-} and major heavy metals included Pb, Cd, Cr, Hg and As. The main objective was to estimate the current water pollution profile of the river. The studied area didn't include the tannery side of the river. As a result, almost all the parameters were within the allowable limit. Also it was safe for industrial use without any kind of treatment.

N. Islam (2018) conducted environmental impact study on Dhaleshwari River due to the shifting of tanneries. CEGIS was assigned to do the study to find out the overall condition of the river. The main objective of the study was to identify the current environmental and social problems. The study identified physical, biological and social issues of the study area. It has been found that water quality of Dhaleshwai River has become the prime concern among all. The effluents of tanneries are affecting both the physical and chemical properties of water. The amount of dissolved oxygen is getting lowered day by day. Heavy metals especially Chromium (Cr) is being disposed from the CETP, which is almost double than the ECR'1997 recommendation of 2 mg/L into inland surface water. As a result, the total ecosystem is facing problems. Many mitigation measures were proposed in the study.

CHAPTER 3

METHODOLOGY

3.1 Introduction

The prime objective of the study is to find out a suitable method for monitoring river water quality. Field measurement and lab testing procedure are costly as well as time consuming process. As the pollution level of Dhaleshwari River is increasing day by day, it is not possible to collect water on a daily basis and testing in the laboratory. Hence, a cost effective and time efficient monitoring technology is desired to protect this river. Currently, the technology of remote sensing has been constantly evolving and can be used to sense river water. The water samples were collected on 18 November 2018 and was taken to environment lab of MIST. Some parameters were tested immediately. It took 5 days to measure all other parameters. After that the images of that particular day were downloaded. ERDAS IMAGINE software was used for extracting the reflectance values. Then the field results and reflectance values were used to generate suitable equations. Then different water indices were measured. Finally, equations are generated with the water indices values. On 18 December, 2018, water samples from the same location was collected and the image of the same location was downloaded again and this time the developed models were used to determine the water quality parameters. The summary of the methodology is given in a flow chart below (figure 3.1):

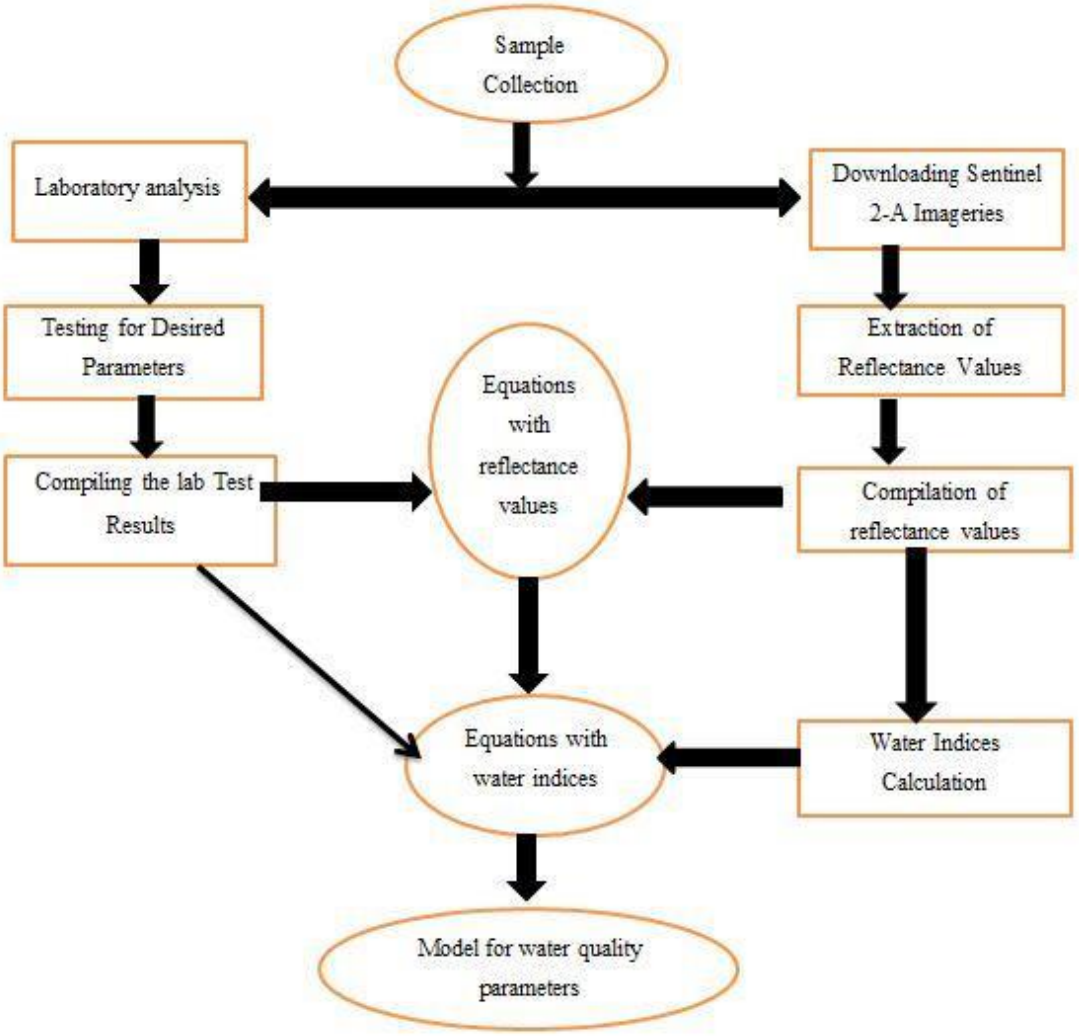

Fig 3.1: Flow chart of methodology

3.2 Field Measurement

10 points along the mid-section of the river were selected for sample collection. The deterioration of the downstream portion of river is also considered in our study. The effluent is directly being discharged into the water. The water condition of the discharge point is very bad. But as it reaches the mid portion of the river it gets diluted with the river water. This water moves downstream of the river. Continuous deterioration of water quality is taking place in the river. A centerline has been chosen for this study. At first preliminary recce was done for fixing the suitable points for sample collection. The CETP (Central Effluent Treatment Plant) is not fully functional yet. As a result, we tried to cover every

significant point of pollution of that area. Water of the other side of river is not being polluted. So we tried to find out the points up to which water is being polluted. 10 such points from upstream to downstream were selected. All the points were approx. near the centerline of river. A local boat was hired for the survey along the river. It took approx. 5 hours to collect sample from every point of the river. Sampling time was approximately 2-3 minutes for every point.

Due to the non-availability of motorized boat, sample collection was very time consuming. A handheld GPS was taken to collect the coordinates (Latitude and Longitude) of the sampling points.

Table 3.1: Coordinates of the selected locations

Point	Lat/Long
1	N 23° 47' 31.7", E 090° 14' 37.8"
2	N 23° 47' 18.3", E 090° 14' 31.6"
3	N 23° 46' 54.1", E 090° 14' 25.4"
4	N 23° 46' 35.9", E 090° 14' 20.9"
5	N 23° 46' 34", E 090° 14' 19.7"
6	N 23° 46' 25.7", E 090° 14' 17.5"
7	N 23° 46' 16.6", E 090° 14' 17.2"
8	N 23° 46' 11.1", E 090° 14' 17.3"
9	N 23° 46' 07.4", E 090° 14' 17.8"
10	N 23° 46' 04.7", E 090° 14' 17.9"

3.3 Sample Collection

Samples were collected following the standard procedures. The necessary items were sample bottles, filtering apparatus, samplers, sample labels, field notebook etc. The sample container was rinsed three times before those were filled. The sample container was labeled

properly by attaching suitable tag. Samples were collected with a weighted bottle. One sample is taken from each point. As it is a flowing river, it was taken from the middle of flowing water. Some determinants like pH and DO get affected easily. pH of a sample keeps changing with time and DO changes during the handling of the samples. The pH value obtained in the laboratory may not be the same as that of water at the time of collection of samples due to loss-or absorption of gases, reactions with sediments, hydrolysis and oxidation or reduction taking place within the sample bottle. Because more O_2 molecules from above the sample surface atmosphere enters sample, increasing it's DO. For this reason, pH and DO were measured immediately after collecting the sample. Rest of the samples was tested in the laboratory.

Fig 3.2: Sample bottles in MIST laboratory

3.4 Laboratory Testing

3.4.1 Determination of pH

pH value is the logarithm of reciprocal of hydrogen ion activity in moles per liter. In water solution, variations in pH value from 7 are mainly due to hydrolysis of salts of strong bases and weak acids or vice-versa. Dissolved gases such as carbon dioxide, hydrogen sulphide and ammonia also affect pH value of water. The overall pH value range of natural water is

generally between 6.5 and 8.5. For the determination of pH electrometricalv method has been used. The test was done using a Milwaukee MW100 Standard Portable pH Meter at 25^0 c room temperature.

At first it was made sure that the pH had been calibrated to the manufacturer's specifications before starting the test. Then the pH meter's probe was rinsed with distilled water and carefully pat dried with a paper towel before each test. It was made sure that nothing was on the probe that can affect the final result of the test. Then a glass container was filled with enough of the test liquid so that the tip of the probe would be fully submerged. It was made sure that the test was performed quickly after adding the liquid to the container as pH levels can shift quickly. The probe was dipped into the test liquid, making sure not to move it around too much.

Fig 3.3: Milwaukee MW100 standard portable pH meter

3.4.2 Determination of DO

Dissolved oxygen (DO) is a relative measure of the amount of oxygen (O_2) dissolved in water. DO is measured either in milligrams per liter (mg/L) or "percent saturation." The standard value of DO set by DOE is 7 mg/L. For the measurement of DO the MW600, a Portable Dissolved Oxygen meter was used. DO levels fluctuate seasonally and over a 24-hour period. They vary with water temperature and altitude. That's why the test was done at the site.

At first, the DO meter was calibrated. Then the meter was adjusted to zero by turning the screw in the middle of the meter. Next, the probe was connected and the meter was turned on for fifteen minutes for optimum performance. After that the redline was adjusted with the control knob to align with the 31 °C (87.8 °F) line and set the central line to 0. All meters are calibrated differently. We saw the manufacturer's instructions for variations that were specific to our meter. Meters were calibrated in Celsius not in Fahrenheit. The samples were taken in beakers. Then the probe was placed into the sample of water. Then we allowed the meter to stabilize. After that the value of DO was taken from the meter. We also checked the sample a few times to make sure the meter was calibrated.

Fig 3.4: The MW600 is a portable Dissolved Oxygen meter

3.4.3 Determination of Color

The spectrophotometry method was used to determine color of the samples. Spectrophotometry is a method to measure how much a chemical substance absorbs light by measuring the intensity of light as a beam of light passes through sample solution. Color is measured by visual comparison of the sample with platinum-cobalt standards (Pt-Co). Color of the sample was determined using the HACH DR 5000 DR5000 Benchtop UV-VIS spectrophotometer. At first the code for determination of color was entered into the machine. After that the machine was calibrated using a 10 ml distilled water solution. Then the sample was taken into another vial and was put inside the machine. Then the value of color was determined by putting the sample inside the machine. We also determined the dilution factor of the samples to calculate the actual color value. This test was done in a room temperature of 23.7ºC.

Fig 3.5: HACH DR 5000 Benchtop UV-VIS Spectrophotometer

3.4.4 Determination of TDS

The mineral concentrations in water are referred as total dissolved solids (TDS). The common measured unit of this is in parts per million (ppm) or mg/l. TDS was determined using the HACH Sension-156 multi-parameter meter at a room temperature of 23.8^0C. For the measurement of TDS, the multi-meter was set at TDS function at first. Then it was calibrated using a clear sample of distilled water. It was made sure that the initial reading was at zero. Then a sample of 50 ml was taken in a beaker and the metal probe was inserted into the sample. The multi-meter automatically showed the amount of TDS present in the sample.

Fig 3.6: HACH Sension 156 multi-parameter meter

3.4.5 Determination of TSS

Total suspended solids (TSS) is the dry-weight of suspended particles that are not dissolved. The common measured unit of this is in parts per million (ppm) or mg/l. The spectrophotometry method was used to determine TSS of the samples. Spectrophotometry

is a method to measure how much a chemical substance absorbs light by measuring the intensity of light as a beam of light passes through sample solution. The standard for this parameter is 25 mg/L (DOE).

TSS of the sample was determined by using HACH DR 5000 DR5000 Benchtop UV-VIS Spectrophotometer. At first, the spectrophotometer was calibrated using a 10ml distilled water sample. Then, before starting the test, all the initial readings were set to zero. For measuring TSS, a required code was entered in the spectrophotometer. After that, a 10 ml test sample was taken in a clear small sized vial and placed inside the machine. After that the readings were automatically generated by the machine and were noted. This whole test was done in a room temperature of 23.7^{o}C.

3.4.6 Determination of Turbidity

It is based on comparison of the intensity of light scattered by the sample under defined conditions with the intensity of light scattered by a standard reference suspension under the same conditions. Turbidity (NTU) of the sample was determined using the APERA instruments TN400 portable turbidity meter. The turbidimeter consists of a nephelometer with a light source for illuminating the sample and one or more photo electric detectors with a readout device to indicate the intensity of light scattered at right angles to the path of the incident light. It is so designed that little stray light will reach the detector in the absence of turbidity and would be free from significant drift after a short warm-up period. At first it was made sure that the turbidity meter had been calibrated to the manufacturer's specifications before starting the tests. Then the vial inside the turbidity meter was filled with the sample and was inserted inside the meter and the read button was pressed. After

the meter stabilized, the value of turbidity was taken. The readings were taken in Nephelometric Turbidity Units and the test was done in a room temperature of 23.7^{o}C.

Fig 3.7: TN400 portable turbidity meter

3.5 Satellite Image Downloading

All Sentinel data are available to the public at no cost from U.S. Geological Survey (USGS) Sentinel images are made of several files or layers (bands) of data. Each band represents a section of the electromagnetic spectrum. The images were downloaded from GloVIS. After registration and account creation, the options for map download were visible in the website. Then after selecting the path-row of the study area, the images of our study area were downloaded. The steps are shown in Fig 3.8-3.10

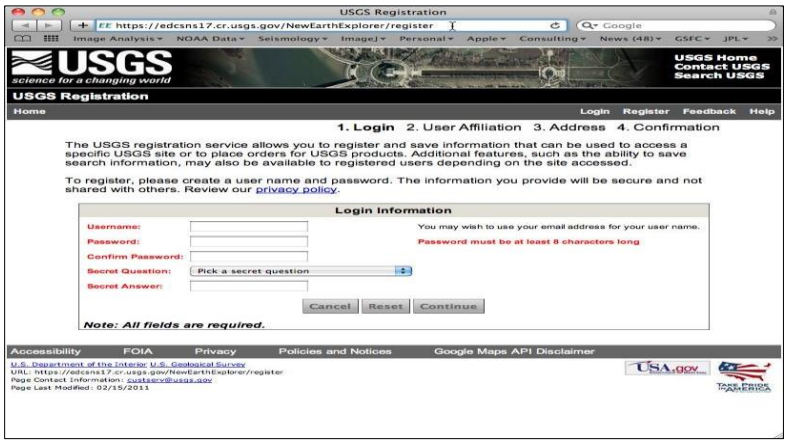

Fig 3.8: Registration interface of USGS

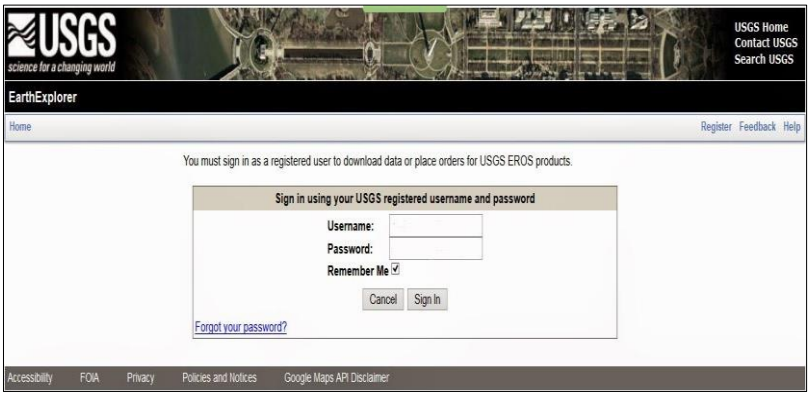

Fig 3.9: Login page of USGS

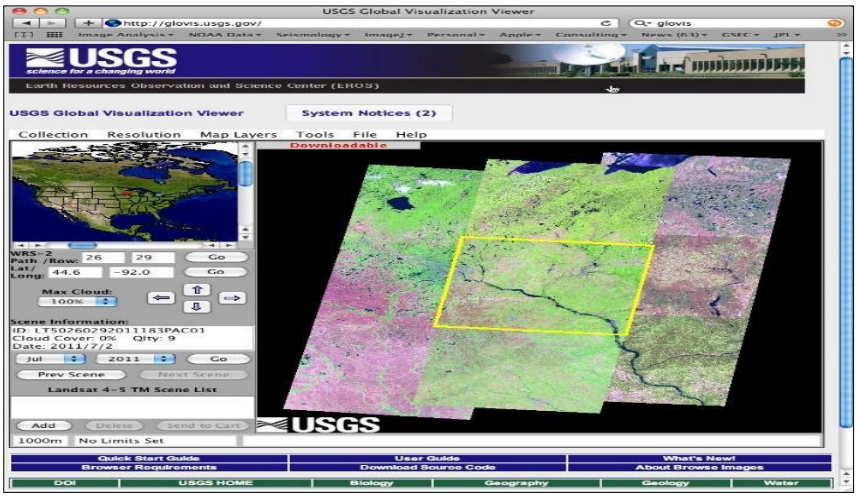

Fig 3.10: USGS (GloVis) website outlook

3.6 Image Processing

For the processing of sentinel-2A image, ERDAS imagine software was used. The images downloaded from the website, were in multiple layers. So stacking was done to merge the bands into a single layer. There are input and output options for selecting desired bands for creating the composite maps. All the options were selected in JPEG format. For this study,11 bands were needed for image creation. Those particular bands were combined to produce a single map. Then finally from the created composite maps, the reflectance values were extracted for all the locations. Detail procedure of image processing is presented in Fig 3.11-3.20 below:

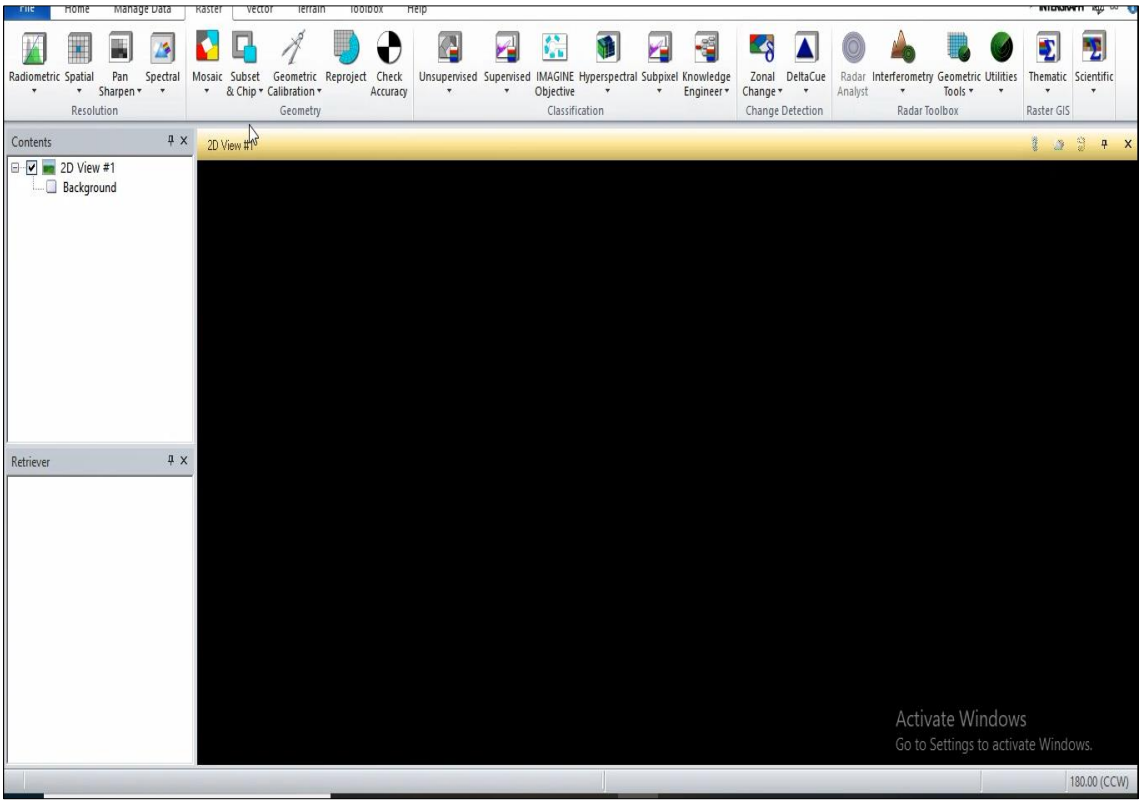

Fig 3.11: Homepage of ERDAS imagine software

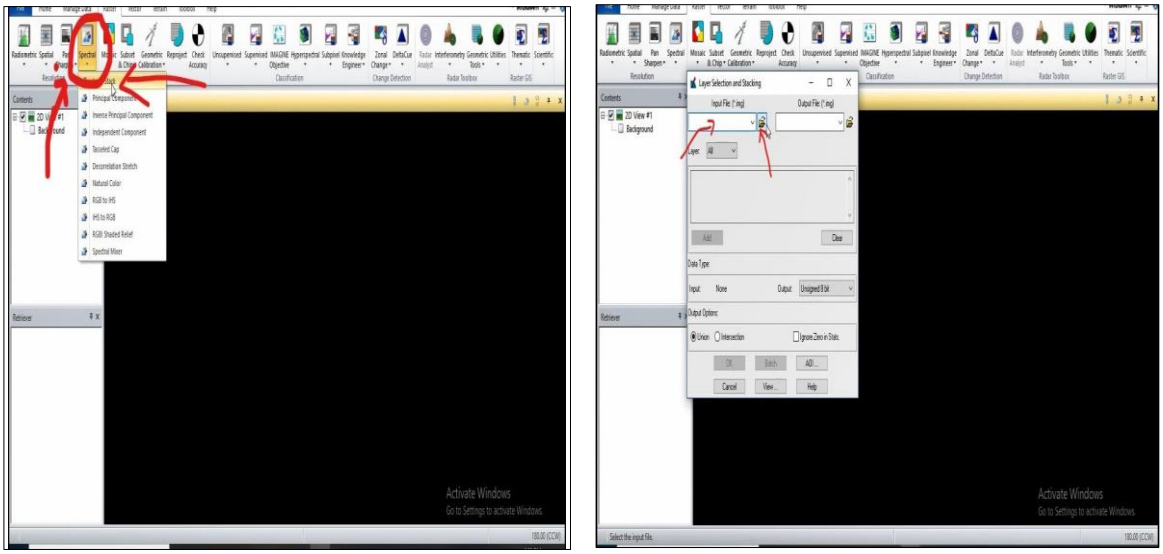

Fig 3.12: Steps of layer selection and stacking

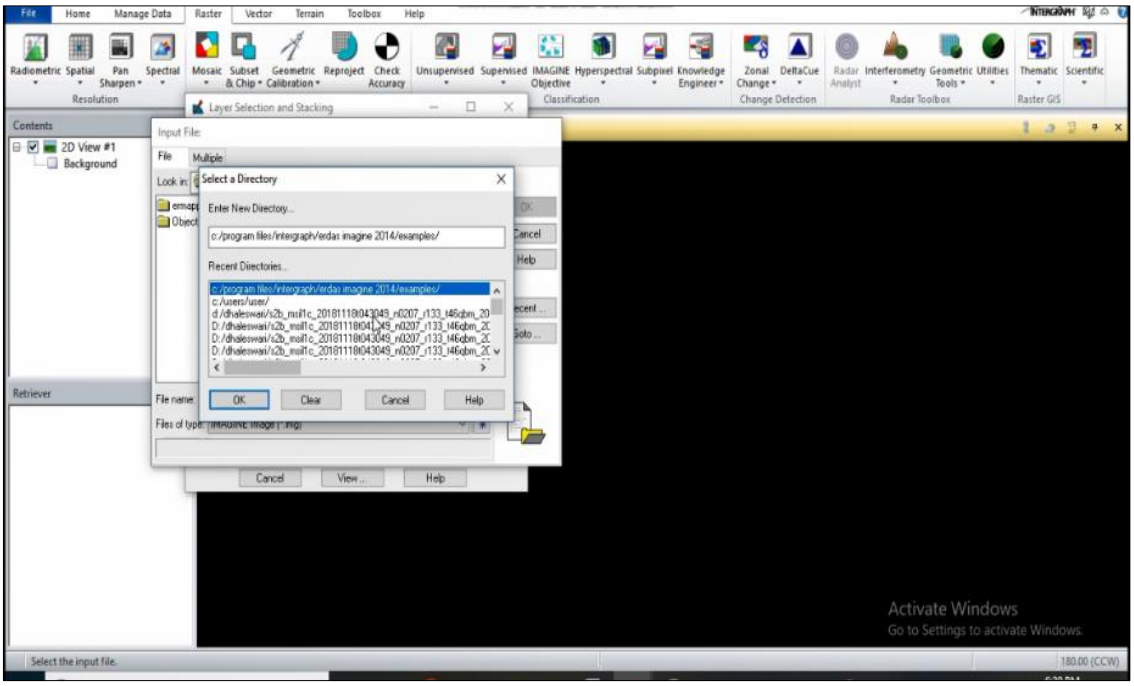

Fig 3.13: Steps of directory selection

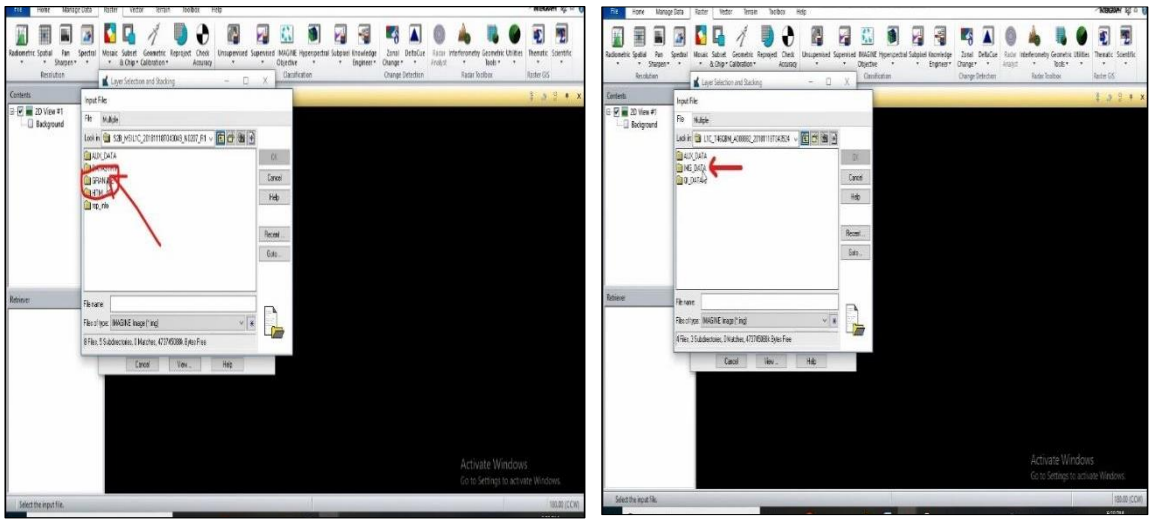

Fig 3.14: Selection of working folder

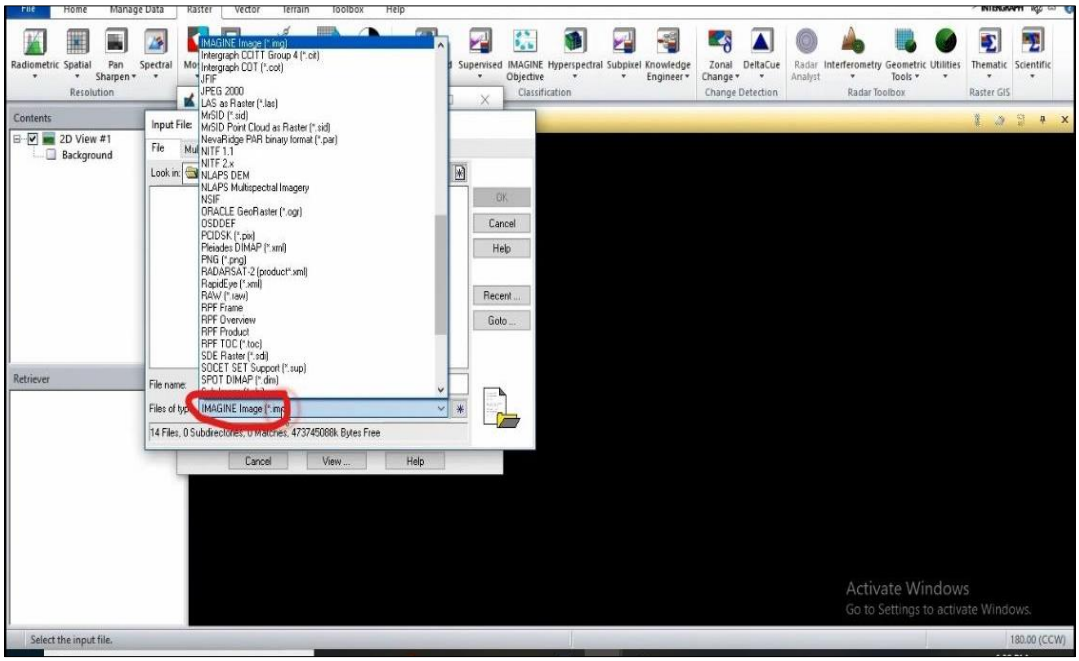

Fig 3.15: Selection of image format

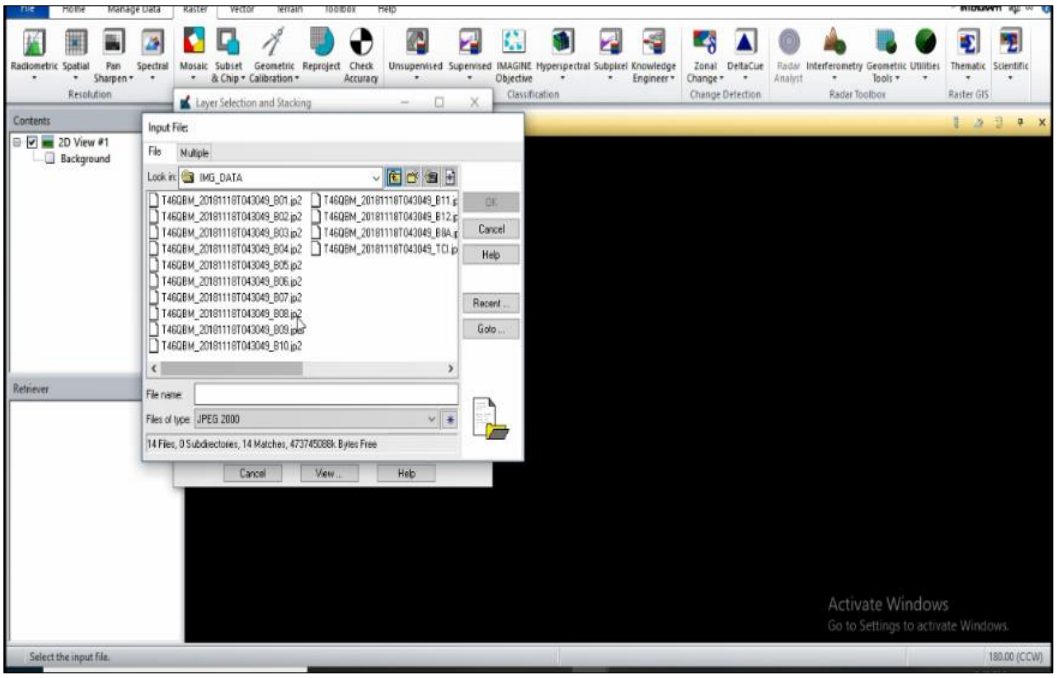

Fig 3.16: Layer selection

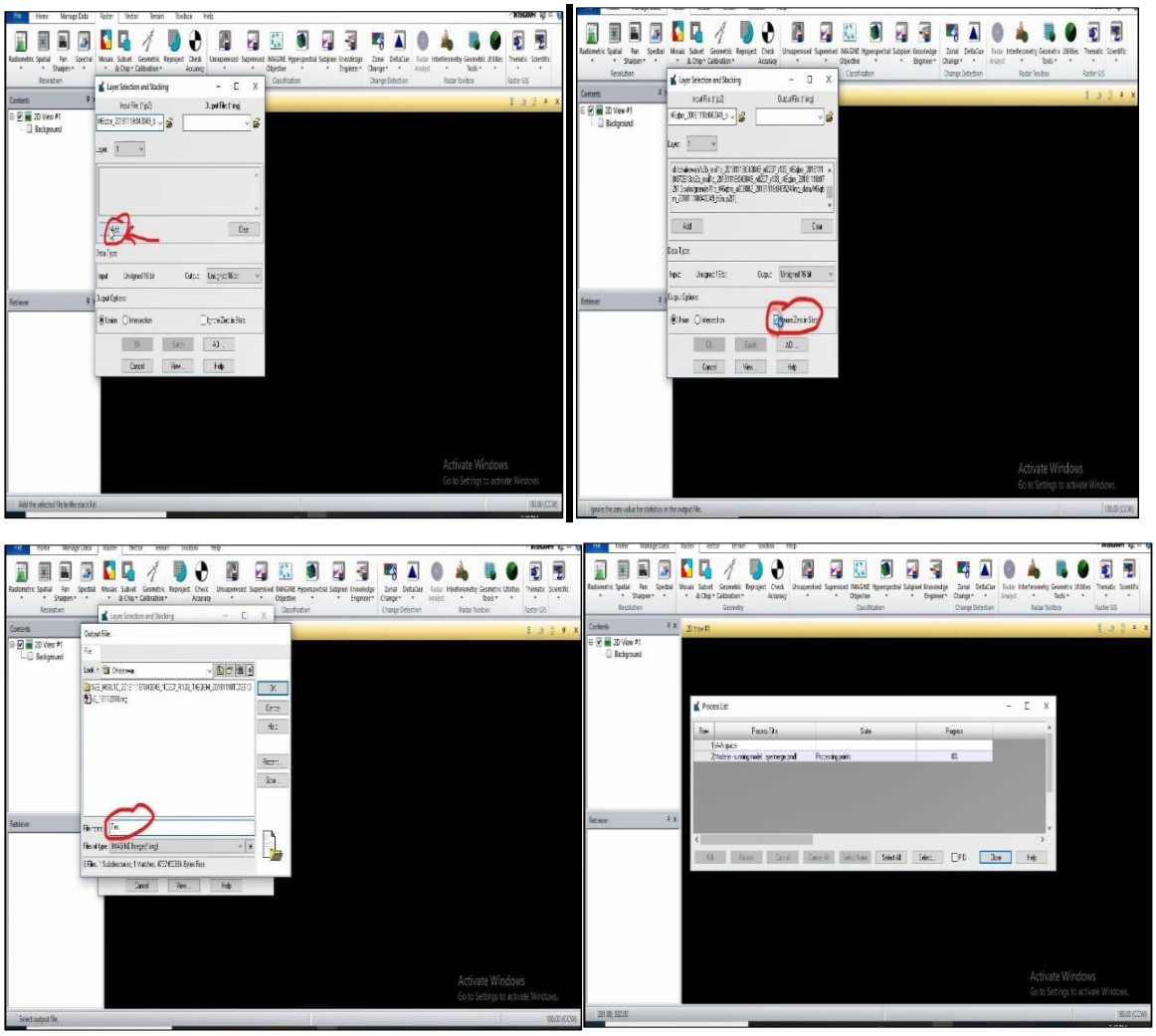

Fig 3.17: Steps of image analysis

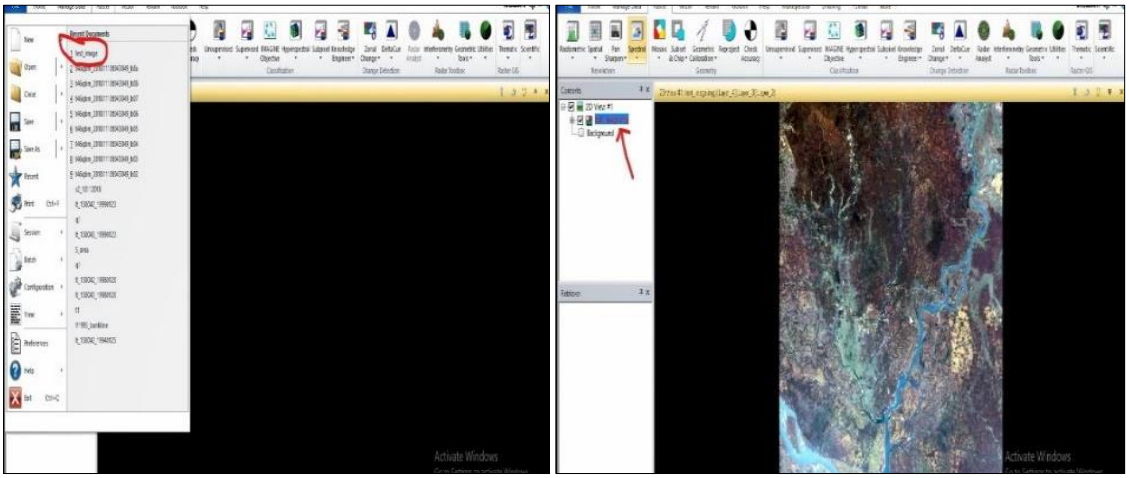

Fig 3.18: Image layer classification.

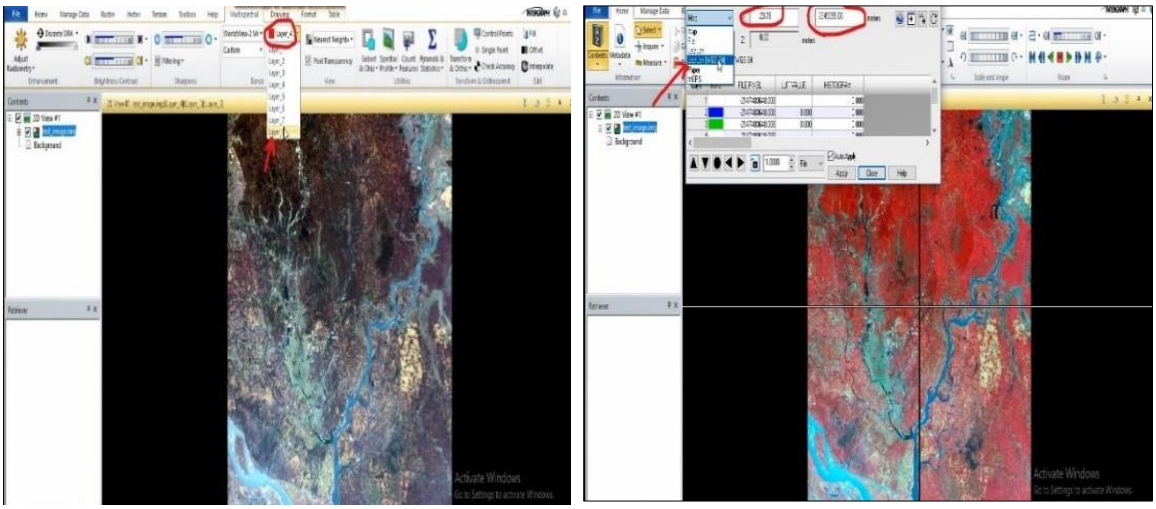

Fig 3.19: Co-ordinate and map selection

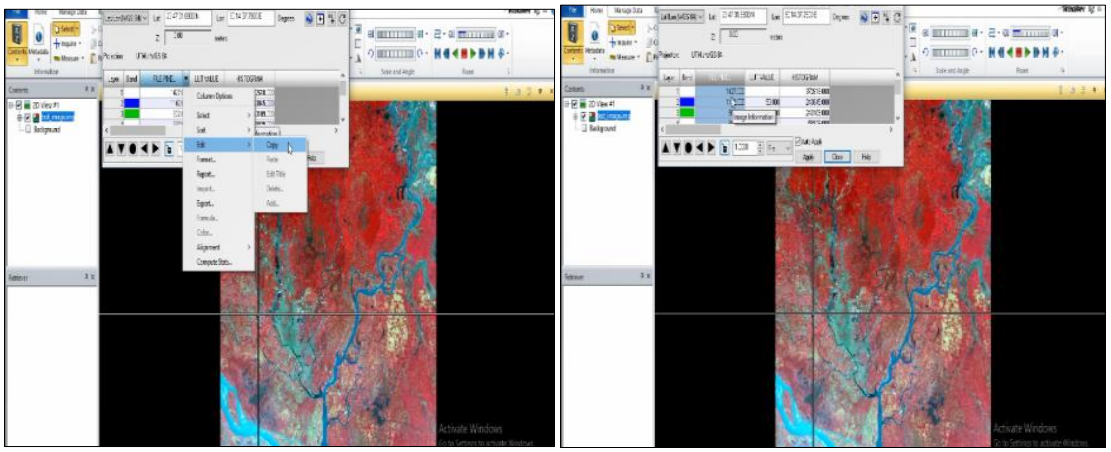

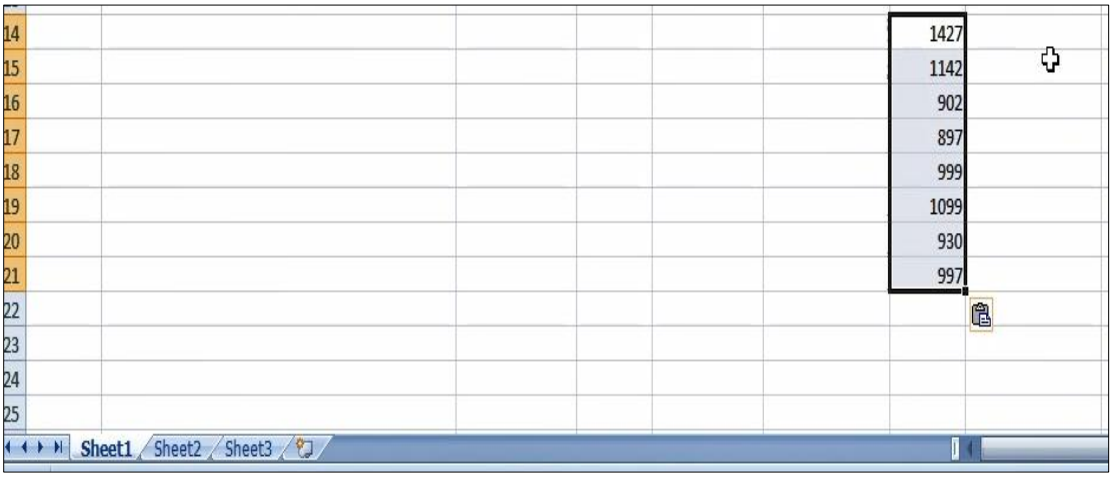

Fig 3.20: Reflectance value extraction

3.7 Index Calculation and Generating Regression Equation

After extracting the reflectance values from the image, those were listed down in an excel datasheet. Among all the 11 band reflectance values, only few were used to calculate the indices. For the calculation of water indices, following equations were used:

Table 3.2: Water indices and their formulas

Index	Formula
Normalized Difference Water Index (NDWI)	$\mathrm{NDWI} = \frac{\mathrm{GREEN} - \mathrm{NIR}}{\mathrm{GREEN} + \mathrm{NIR}}$
Modification of Normalized Difference Water Index (MNDWI)	$\mathrm{MNDWI} = \frac{\mathrm{GREEN} - \mathrm{SWIR2}}{\mathrm{GREEN} + \mathrm{SWIR2}}$
Normalized Difference Moisture Index (NDMI)	$\mathrm{NDMI} = \frac{\mathrm{RED} - \mathrm{NIR}}{\mathrm{RED} + \mathrm{NIR}}$
Automated Water Extraction Index (AWEI)	$\mathrm{AWEI} = 4 * (\mathrm{GREEN} - \mathrm{SWIR2}) - (0.25 * \mathrm{NIR} + 2.75 * \mathrm{SWIR1})$
Water Ratio Index (WRI)	$\mathrm{WRI} = \frac{\mathrm{GREEN} + \mathrm{RED}}{\mathrm{NIR} + \mathrm{SWIR2}}$

From the equations, it can be seen that only Red, Green, NIR, SWIR1 and SWIR2 band reflectance values are needed. According to Sentinel-2A image classification- Band 4 is Red, Band 3 is Green, Band 8 is NIR and Band 11 and Band 12 are respectively SWIR1 and SWIR2. After separating these bands, water indices were calculated using the formulas given in Table 3.2.

After calculating the water indices, they were used in multiple regression analysis. Using each index separately with the parameters or by using multiple indices with the quality parameters, regression models were formed. Whole regression analysis was done in Microsoft Excel.

For the multiple regression analysis, the “Regression” function under the “Data analysis” tab was used. For the selection of data, all the index values were selected as “X- axis” values and the quality parameter values were selected as values of “Y-axis”.

Finally, an image of 18 December, 2018 of the same location was downloaded again and the reflectance value of that day for selected five locations were extracted using the same method. Then water indices were calculated using the same formula and the values were applied on the developed model. Thus, we obtained a new set of water quality parameter data. Water samples of that 5 locations from Dhaleshwari river was collected on 18 December, 2018 and tested in the laboratory. Then the field values were compared with the model derived values to validate the models.

CHAPTER 4

RESULTS AND DISCUSSION

4.1 Introduction

This section represents the main results from field investigations and satellite data. Chronologically field data, linear equations from reflectance values and equations from water indices have been illustrated here. Discussion includes comparison between field data results, and both types of equations.

4.2 Field Data

A total number of 10 samples were collected and tested in the laboratory. The water quality parameters obtained from the laboratory tests for each location is given below:

Table 4.1: Laboratory test results for different locations

Location	pH	DO	TDS	TSS	Turbidity	Color
1	7.21	3.2	347	17	6.81	28
2	7.06	1.7	416	14	6.72	63
3	7.05	2.4	387	15	5.32	42
4	6.93	1.8	408	13	4.52	38
5	6.88	2.8	409	16	6.21	51
6	6.88	2.2	427	12	5.21	38
7	6.83	1.3	441	11	4.3	35
8	6.86	1.6	433	18	7	39
9	6.81	1.1	440	15	6.21	34
10	6.82	2	499	13	3.2	40

4.3 Generating Equations

4.3.1 Correlation Results

On the first day we took 10 samples from 10 different locations. The reflectance values obtained from image analysis is given below:

Table 4.2: Reflectance values for selected locations

Location	Band 2	Band 3	Band 4	Band 5	Band 6	Band 7	Band 8	Band 8A
1	1427	1142	902	897	999	1099	930	997
2	1451	1166	932	864	1004	1026	960	947
3	1440	1124	901	853	990	985	908	913
4	1436	1133	899	884	1055	1039	905	1014
5	1453	1149	921	890	965	1051	952	1013
6	1429	1147	909	866	961	1048	944	1016
7	1423	1148	913	889	1032	1119	949	1021
8	1434	1153	928	895	1051	1112	1000	1047
9	1441	1163	907	915	1067	1145	1005	984
10	1417	1138	891	880	1047	1151	956	1056

4.3.2 Correlation Between pH and Reflectance value

The correlation graph between pH and all the color bands are given below:

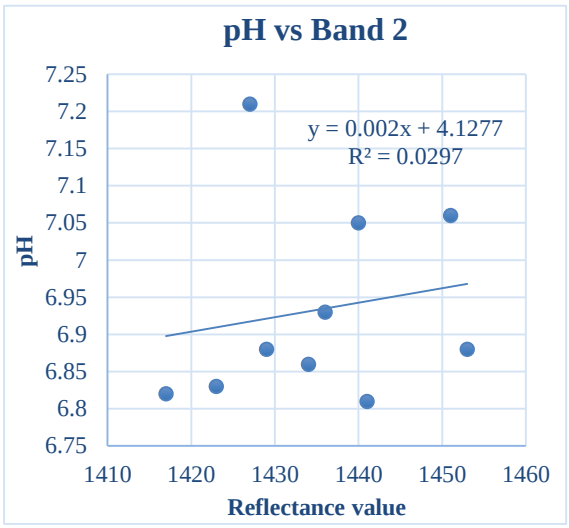

Fig 4.1: Correlation graph pH vs Band 2 reflectance value

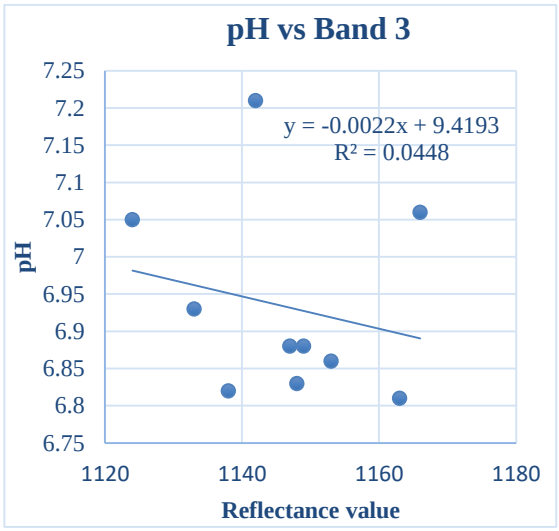

Fig 4.2: Correlation graph pH vs Band 3 reflectance value

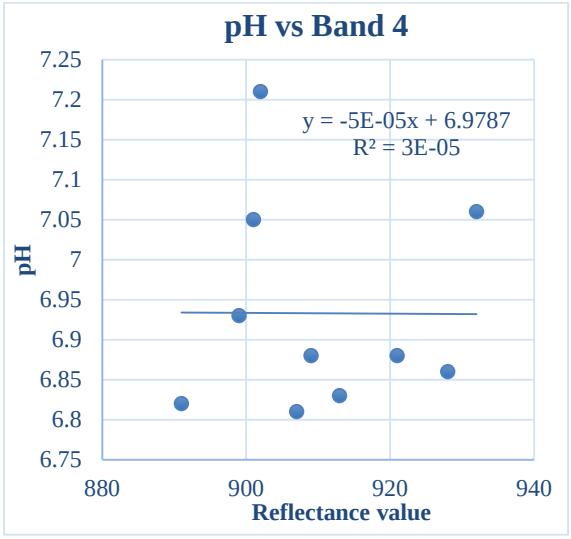

Fig 4.3: Correlation graph pH vs Band 4 reflectance value

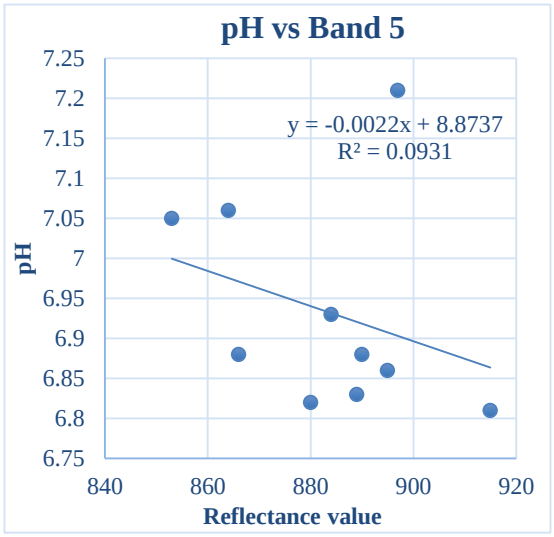

Fig 4.4: Correlation graph pH vs Band 5 reflectance value

The generated equations and corresponding regression values are given in Table 4.3:

Table 4.3: Generated equations and regression values-1 (pH)

Graph No. and Name	Generated Equation	Regression
Fig 4.1 - pH vs Band 2	y = 0.002x + 4.1277	R^2 = 0.0297
Fig 4.2 - pH vs Band 3	y = -0.0022x + 9.4193	R^2 = 0.0448
Fig 4.3 - pH vs Band 4	y = -5E-05x + 6.9787	R^2 = 3E-05
Fig 4.4 - pH vs Band 5	y = -0.0022x + 8.8737	R^2 = 0.0931

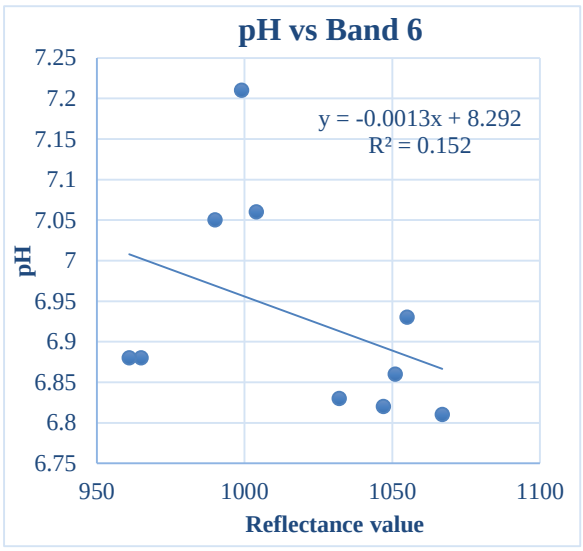

Fig 4.5: Correlation graph pH vs Band 6 reflectance value

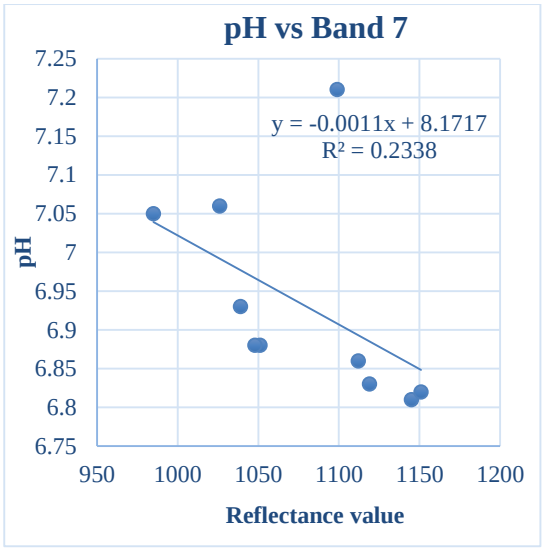

Fig 4.6: Correlation graph pH vs Band 7 reflectance value

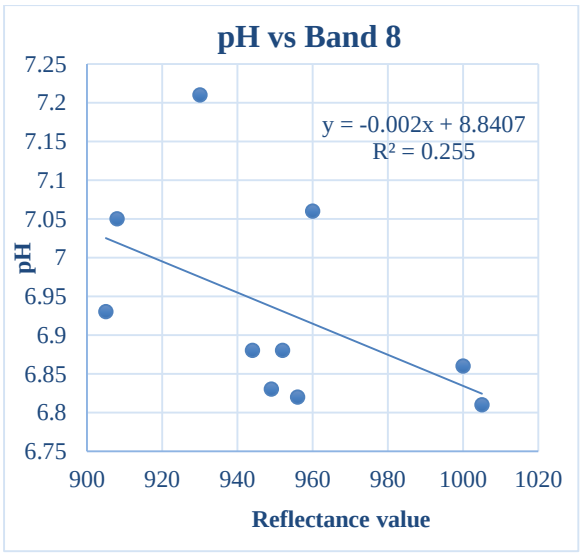

Fig 4.7: Correlation graph pH vs Band 8 Reflectance value

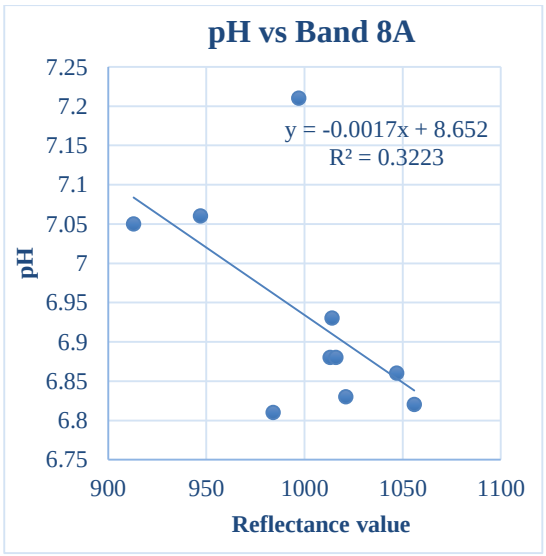

Fig 4.8: Correlation graph pH vs Band 8A Reflectance value

The generated equations and corresponding regression values are given in Table 4.4:

Table 4.4: Generated equations and regression values-2 (pH)

Graph No. and Name	Generated Equation	Regression
Fig 4.5 - pH vs Band 6	y = -0.0013x + 8.292	R^2 = 0.152
Fig 4.6 - pH vs Band 7	y = -0.0011x + 8.1717	R^2 = 0.2338
Fig 4.7 - pH vs Band 8	y = -0.002x + 8.8407	R^2 = 0.255
Fig 4.8 - pH vs Band 8A	y = -0.0017x + 8.652	R^2 = 0.3223

4.3.3 Correlation between DO and Reflectance Values

The correlation graph between DO and all the color bands are given below:

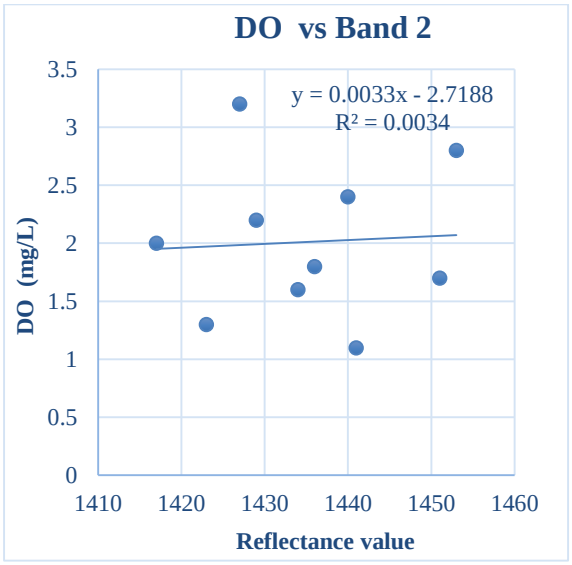

Fig 4.9: Correlation graph DO vs Band 2 reflectance value

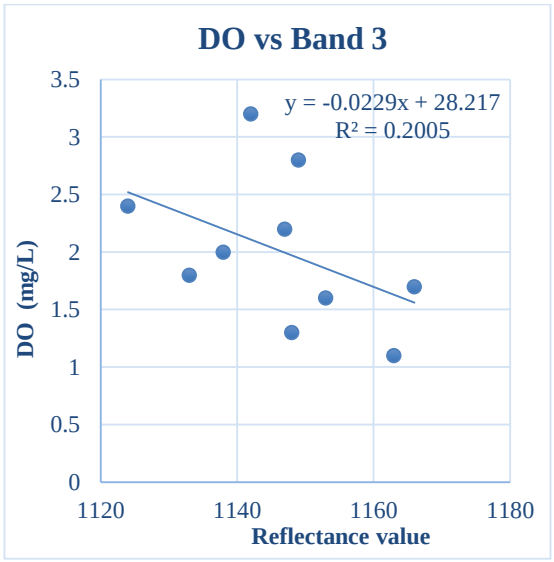

Fig 4.10: Correlation graph DO vs Band 3 reflectance value

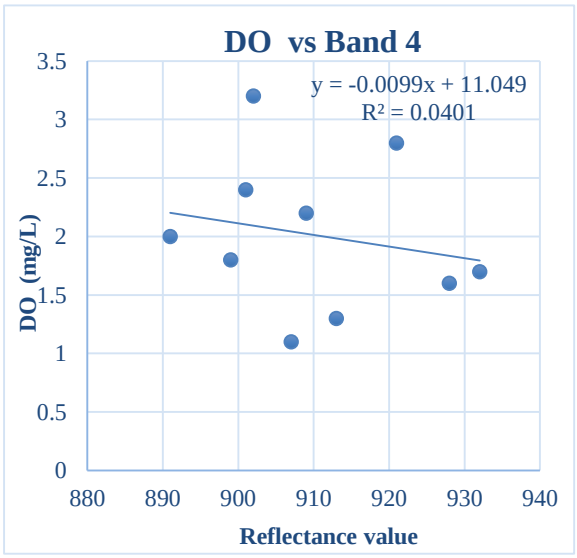

Fig 4.11: Correlation graph DO vs Band 4 reflectance value

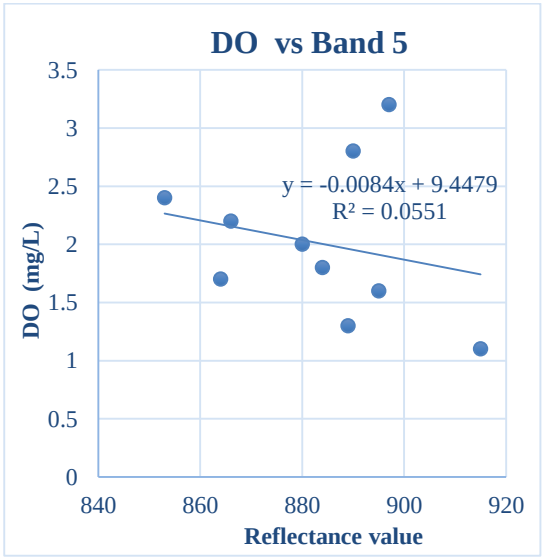

Fig 4.12: Correlation graph DO vs Band 5 reflectance value

The generated equations and corresponding regression values are given in Table 4.5:

Table 4.5: Generated equations and regression values-1 (DO)

Graph No. and Name	Generated Equation	Regression
Fig 4.9 - DO vs Band 2	y = 0.0033x - 2.7188	R^2 = 0.0034
Fig 4.10 - DO vs Band 3	y = -0.0229x + 28.217	R^2 = 0.2005
Fig 4.11 - DO vs Band 4	y = -0.0099x + 11.049	R^2 = 0.0401
Fig 4.12 - DO vs Band 5	y = -0.0084x + 9.4479	R^2 = 0.0551

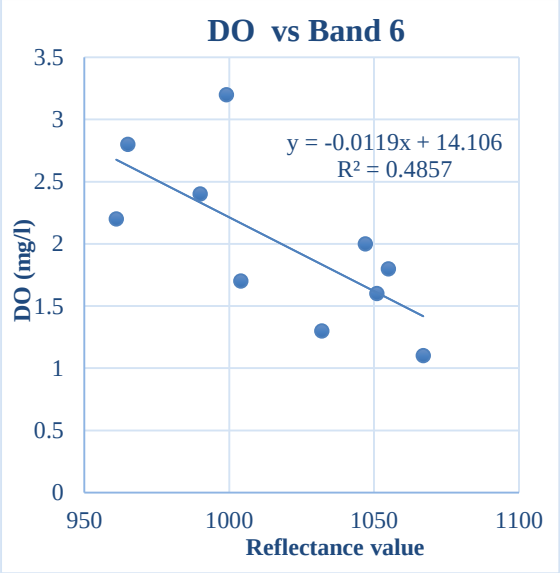

Fig 4.13: Correlation graph DO vs Band 6 reflectance value

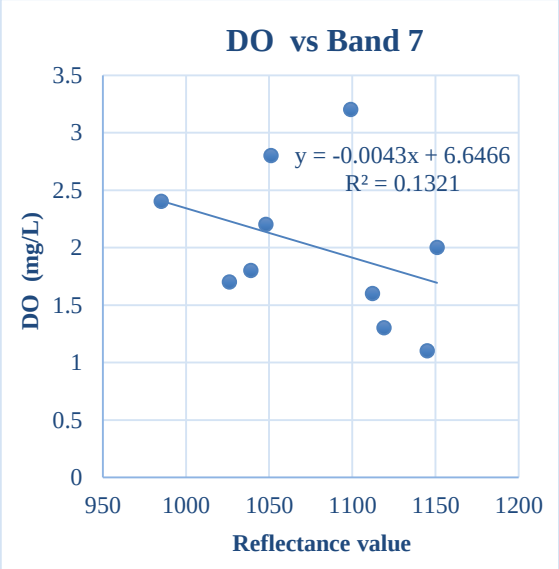

Fig 4.14: Correlation graph DO vs Band 7 reflectance value

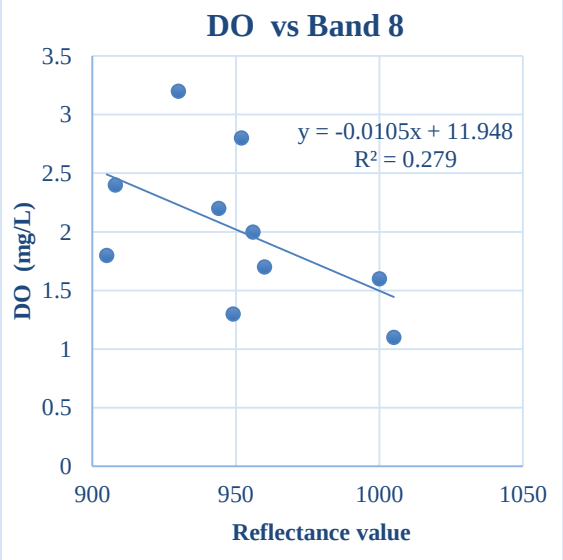

Fig 4.15: Correlation graph DO vs Band 8 reflectance value

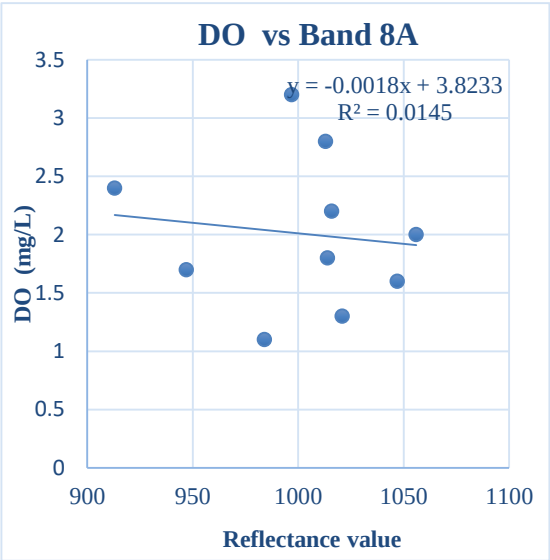

Fig 4.16: Correlation graph DO vs Band 8A reflectance value

The generated equations and corresponding regression values are given in Table 4.6:

Table 4.6: Generated equations and regression values-2 (DO)

Graph No. and Name	Generated Equation	Regression
Fig 4.13 - DO vs Band 6	y = -0.0119x + 14.106	R^2 = 0.4857
Fig 4.14 - DO vs Band 7	y = -0.0043x + 6.6466	R^2 = 0.1321
Fig 4.15 - DO vs Band 8	y = -0.0105x + 11.948	R^2 = 0.279
Fig 4.16 - DO vs Band 8A	y = -0.0018x + 3.8233	R^2 = 0.0145

4.3.4 Correlation Between TDS and Reflectance Values

The correlation graph between TDS and all the color bands are given below:

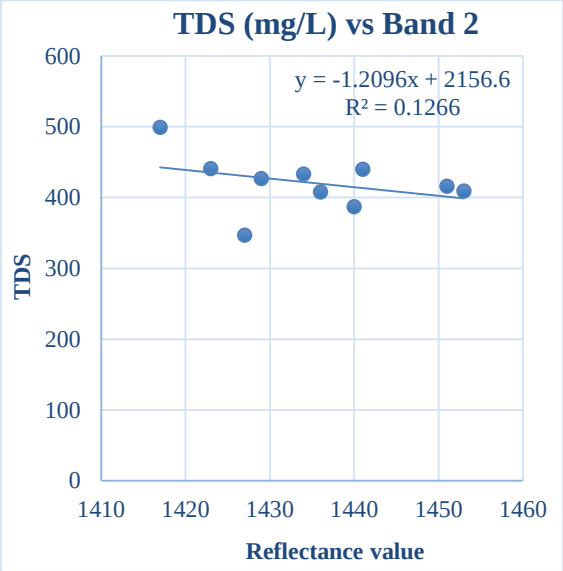

Fig. 4.17: Correlation graph TDS vs Band 2 reflectance value

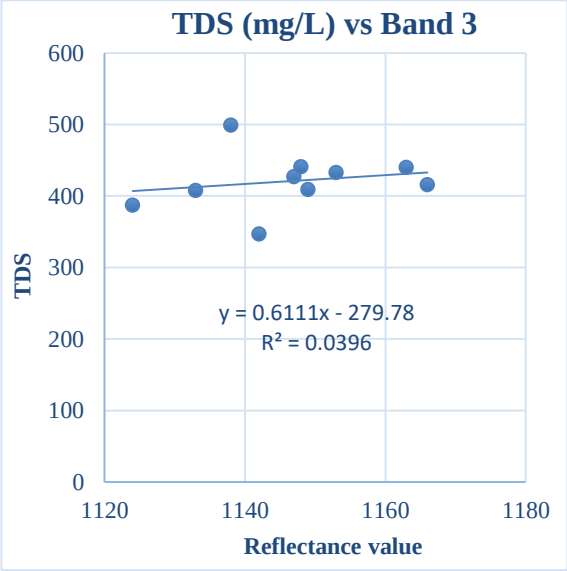

Fig. 4.18: Correlation graph TDS vs Band 3 reflectance value

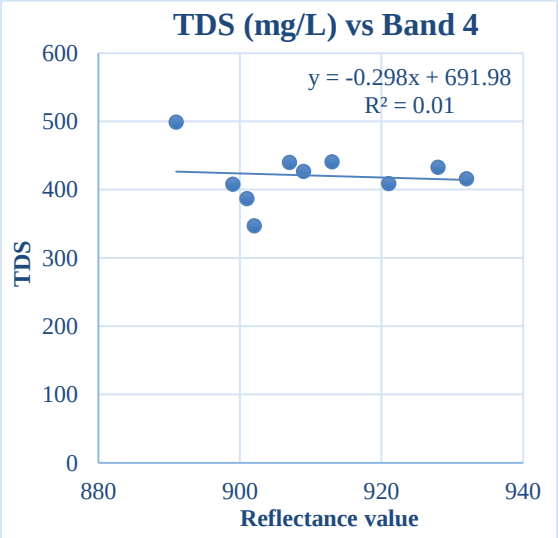

Fig. 4.19: Correlation graph TDS vs Band 4 reflectance value

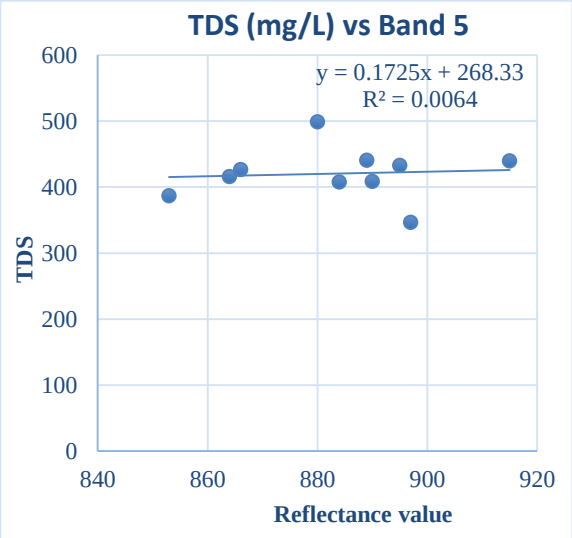

Fig. 4.20: Correlation graph TDS vs Band 5 reflectance value

The generated equations and corresponding regression values are given in Table 4.7:

Table 4.7: Generated equations and regression values-1 (TDS)

Graph No. and Name	Generated Equation	Regression
Fig 4.25 - TDS vs Band 2	y = -1.2096x + 2156.6	R^2 = 0.1266
Fig 4.26 - TDS vs Band 3	y = 0.6111x - 279.78	R^2 = 0.0396
Fig 4.27- TDS vs Band 4	y = -0.298x + 691.98	R^2 = 0.01
Fig 4.28 – TDS vs Band 5	y = 0.1725x + 268.33	R^2 = 0.0064

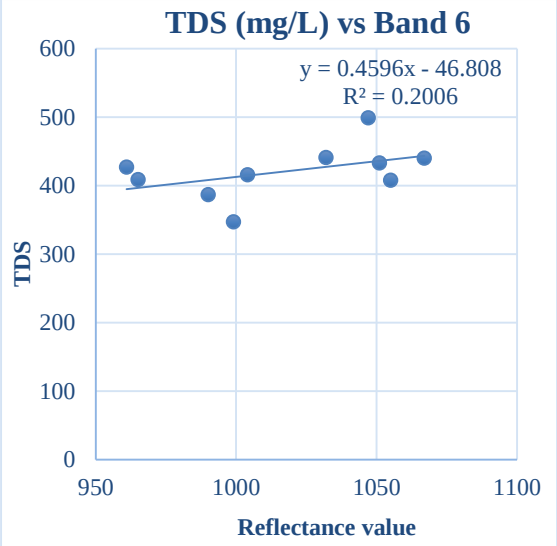

Fig. 4.21: Correlation graph TDS vs Band 6 reflectance value

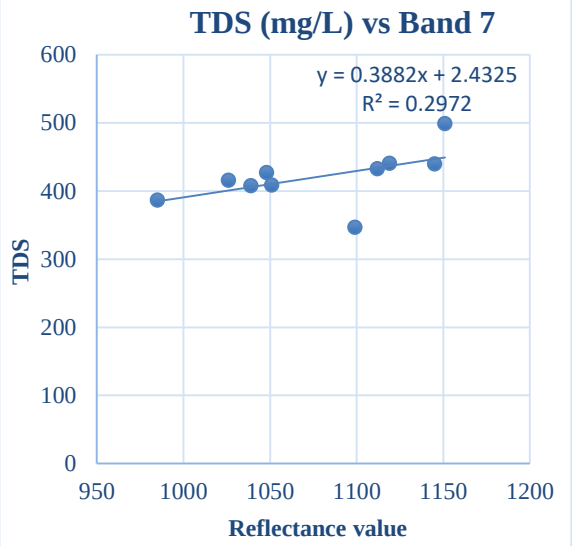

Fig. 4.22: Correlation graph TDS vs Band 7 reflectance value

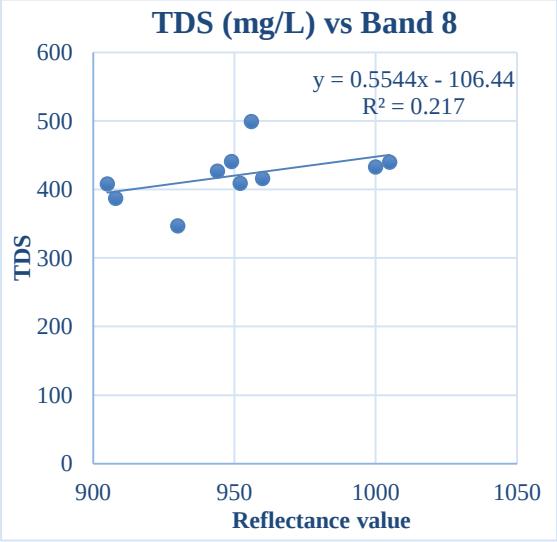

Fig. 4.23: Correlation graph TDS vs Band 8 reflectance value

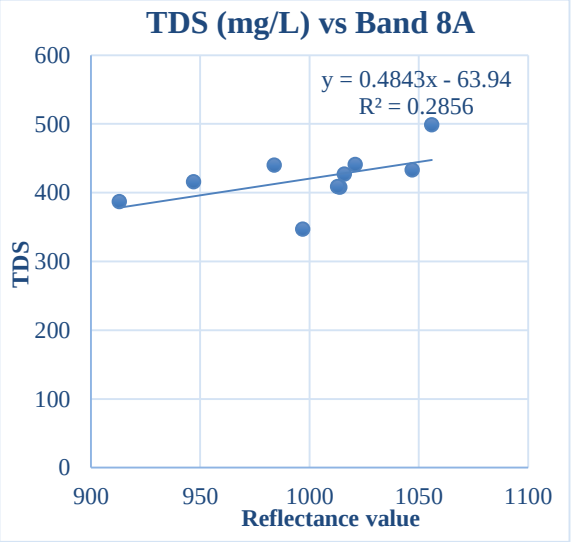

Fig. 4.24: Correlation graph TDS vs Band 8A reflectance value

The generated equations and corresponding regression values are given in Table 4.8:

Table 4.8: Generated equations and regression values-2 (TDS)

Graph No. and Name	Generated Equation	Regression
Fig 4.29 - TDS vs Band 6	y = 0.4596x - 46.808	R^2 = 0.2006
Fig 4.30 - TDS vs Band 7	y = 0.3882x + 2.4325	R^2 = 0.2972
Fig 4.27 - TDS vs Band 8	y = 0.5544x - 106.44	R^2 = 0.2170
Fig 4.28 - TDS vs Band 8A	y = 0.4843x - 63.940	R^2 = 0.2856

4.3.5 Correlation Between TSS and Reflectance Values

The correlation graph between TSS and all the color bands are given below:

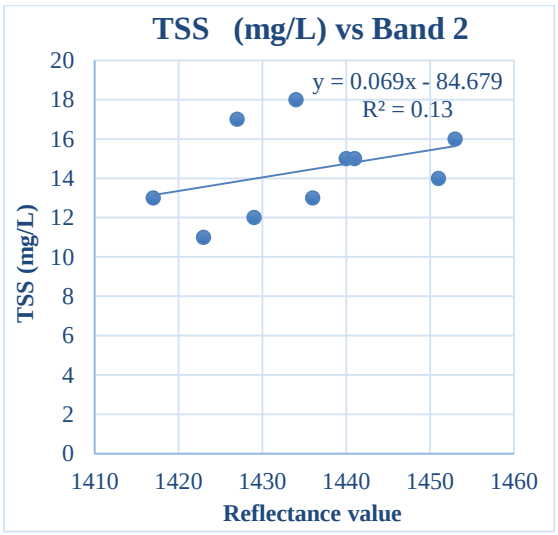

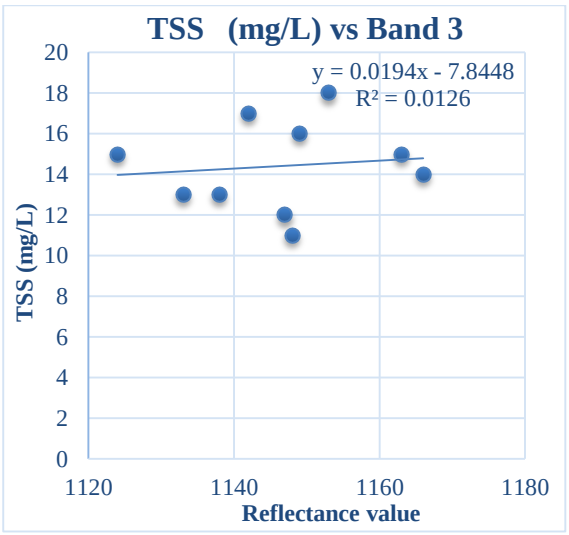

Fig 4.25: Correlation graph TSS vs Band 2 reflectance value **Fig 4.26: Correlation graph TSS vs Band 3 reflectance value**

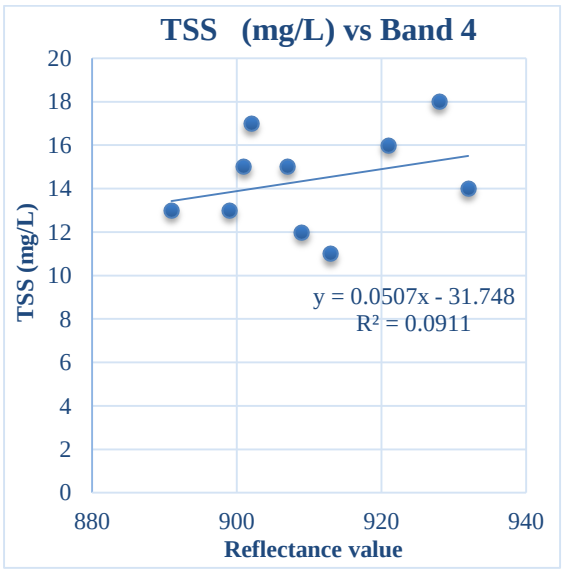

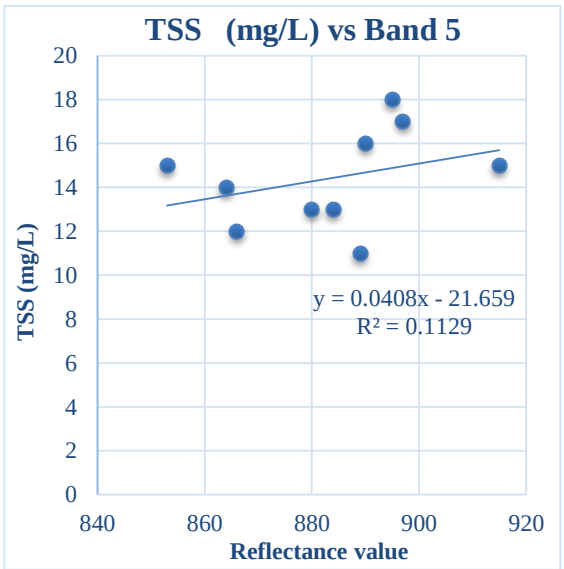

Fig 4.27: Correlation graph TSS vs Band 4 reflectance value **Fig 4.28: Correlation graph TSS vs Band 5 reflectance value**

The generated equations and corresponding regression values are given in Table 4.9:

Table 4.9: Generated equations and regression values-1 (TSS)

Graph No. and Name	Generated Equation	Regression
Fig 4.33 - TSS vs Band 2	y = 0.069x - 84.679	R^2 = 0.13
Fig 4.34- TSS vs Band 3	y = 0.0194x - 7.8448	R^2 = 0.0126
Fig 4.35 - TSS vs Band 4	y = 0.0507x - 31.748	R^2 = 0.0911
Fig 4.36 - TSS vs Band 5	y = 0.0408x - 21.659	R^2 = 0.1129

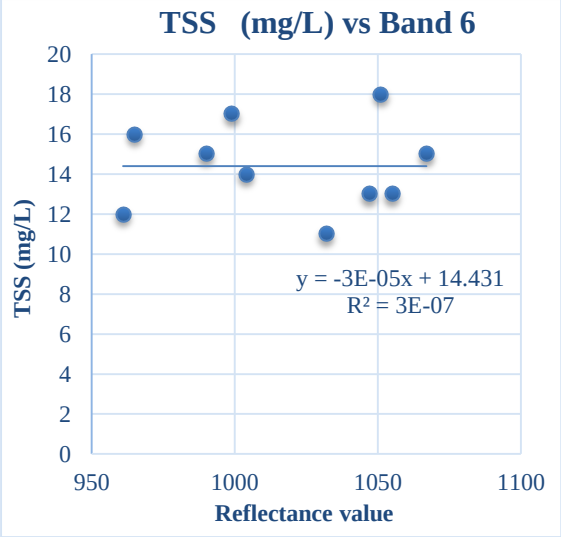

Fig 4.29: Correlation graph TSS vs Band 6 reflectance value

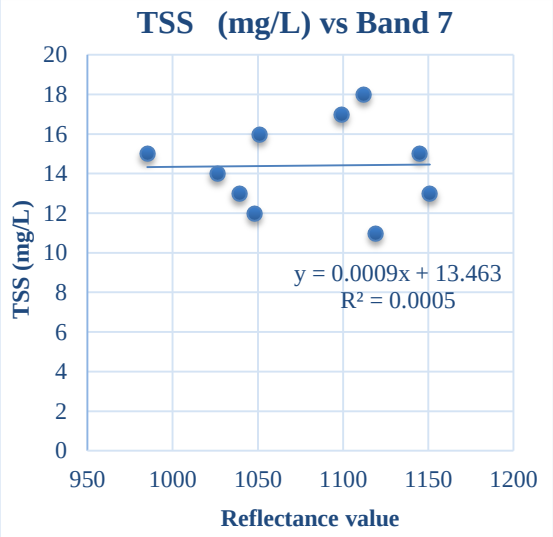

Fig 4.30: Correlation graph TSS vs Band 7 reflectance value

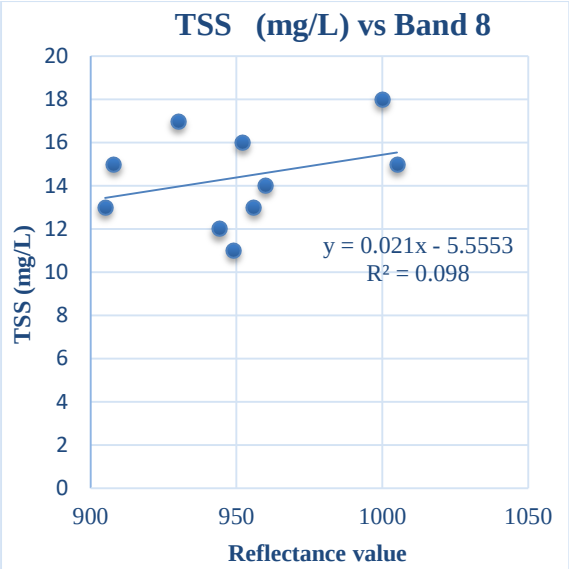

Fig 4.31: Correlation graph TSS vs Band 8 reflectance value

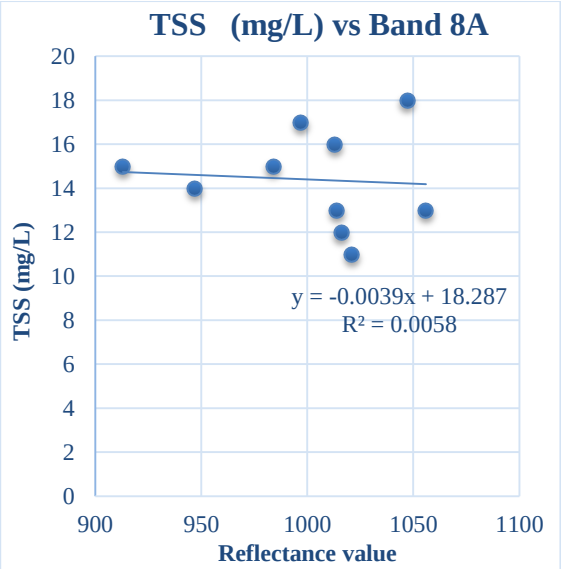

Fig 4.32: Correlation graph TSS vs Band 8A reflectance value

The generated equations and corresponding regression values are given in Table 4.10:

Table 4.10: Generated equations and regression values-2 (TSS)

Graph No. and Name	Generated Equation	Regression
Fig 4.37 - TSS vs Band 6	y = -3E-05x + 14.431	R² = 3E-07
Fig 4.38- TSS vs Band 7	y = 0.0009x + 13.463	R² = 0.0005
Fig 4.39 - TSS vs Band 8	y = 0.021x - 5.5553	R² = 0.098
Fig 4.40 - TSS vs Band 8A	y = -0.0039x + 18.287	R² = 0.0058

4.3.6 Correlation Between Turbidity and Reflectance Values

The correlation graph between Turbidity and all the color bands are given below:

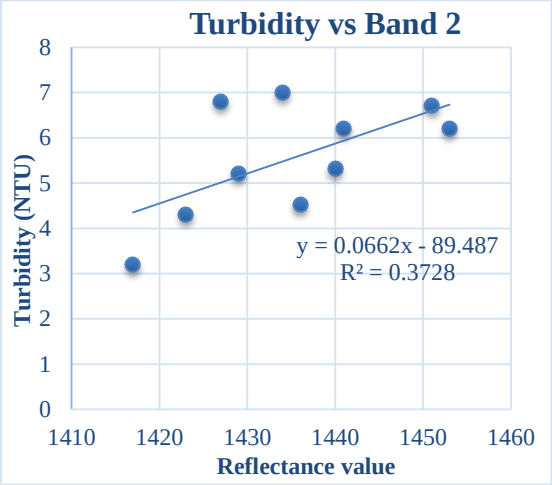

Fig 4.33: Correlation graph Turbidity vs Band 2 reflectance

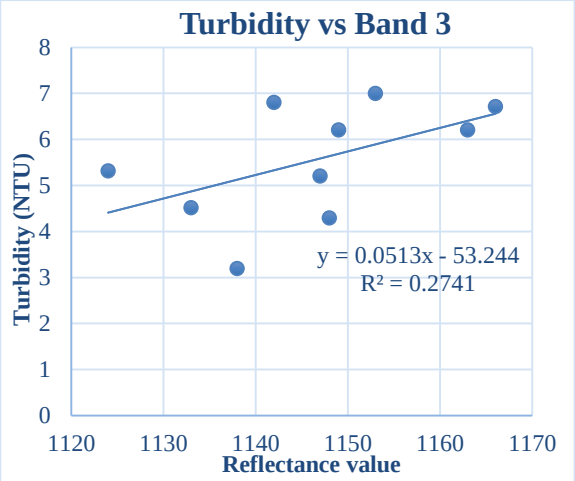

Fig 4.34: Correlation graph Turbidity vs Band 3 reflectance

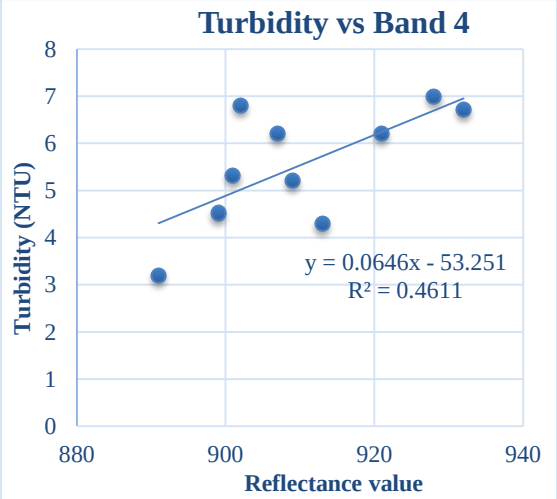

Fig 4.35: Correlation graph Turbidity vs Band 4 reflectance

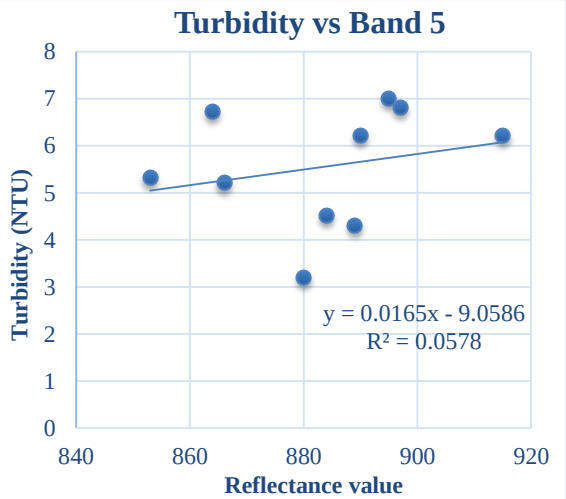

Fig. 4.36: Correlation graph Turbidity vs Band 5 reflectance

The generated equations and corresponding regression values are given in Table 4.11:

Table 4.11: Generated equations and regression values-1 (Turbidity)

Graph No. and Name	Generated Equation	Regression
Fig 4.41 - Turbidity vs Band 2	y = 0.0662x - 89.487	R^2 = 0.3728
Fig 4.42- Turbidity vs Band 3	y = 0.0513x - 53.244	R^2 = 0.2741
Fig 4.43 – Turbidity vs Band 4	y = 0.0646x - 53.251	R^2 = 0.4611
Fig 4.44 - Turbidity vs Band 5	y = 0.0165x - 9.0586	R^2 = 0.0578

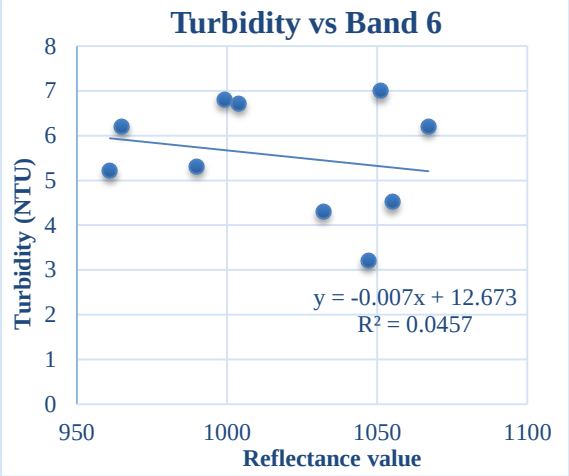

Fig. 4.37: Correlation graph Turbidity vs Band 6 reflectance

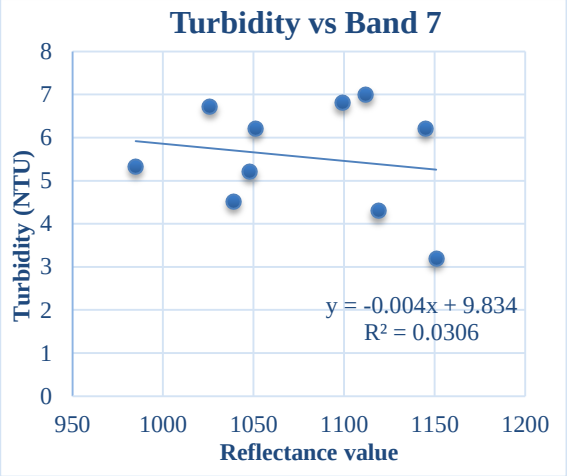

Fig. 4.38: Correlation graph Turbidity vs Band 7 reflectance

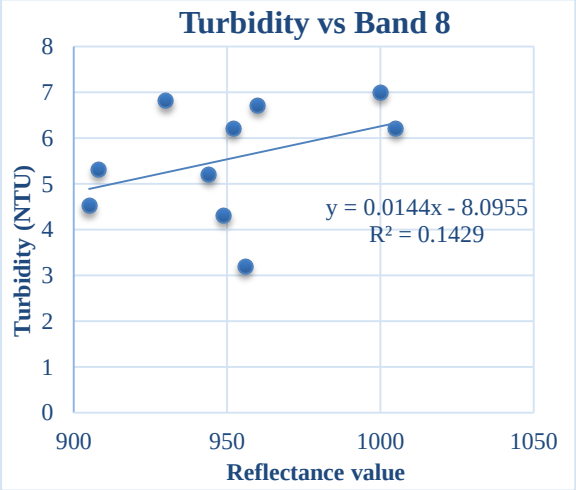

Fig. 4.39: Correlation graph Turbidity vs Band 8 reflectance

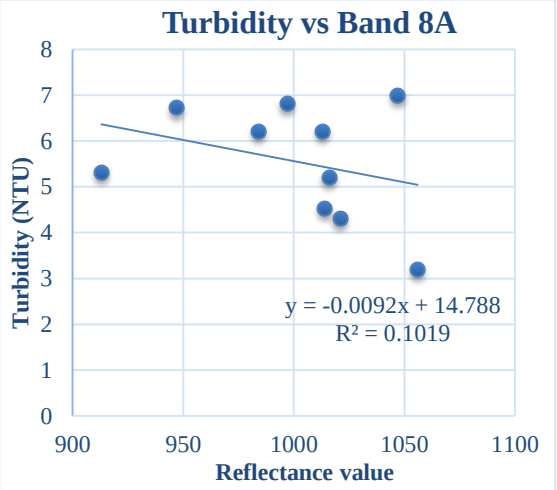

Fig. 4.40: Correlation graph Turbidity vs Band 8A reflectance

The generated equations and corresponding regression values are given in Table 4.12:

Table 4.12: Generated equations and regression values-2 (Turbidity)

Graph No. and Name	Generated Equation	Regression
Fig 4.45 - Turbidity vs Band 6	y = -0.007x + 12.673	R^2 = 0.0457
Fig 4.46- Turbidity vs Band 7	y = -0.004x + 9.834	R^2 = 0.0306
Fig 4.47 – Turbidity vs Band 8	y = 0.0144x - 8.0955	R^2 = 0.1429
Fig 4.48 - Turbidity vs Band 8A	y = -0.0092x + 14.788	R^2 = 0.1019

4.3.7 Correlation Between Color and Reflectance Values

Now the correlation graph between Color and all the color bands are given below:

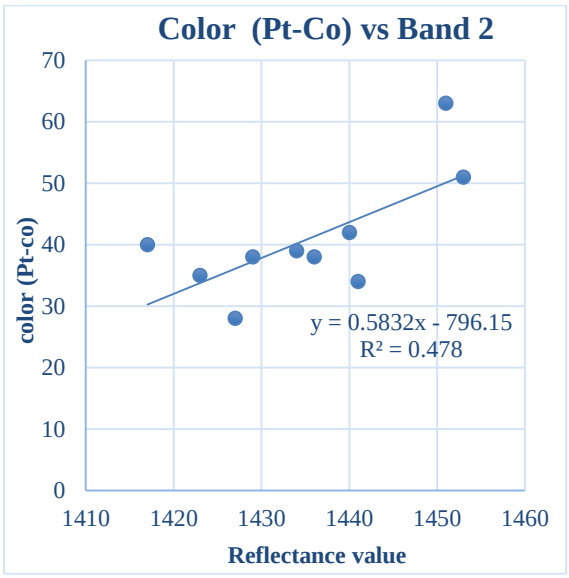

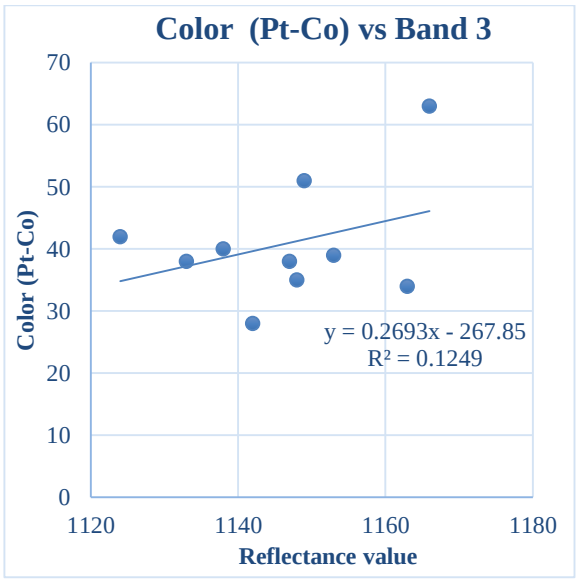

Fig 4.41: Correlation graph Color vs Band 2 reflectance value **Fig 4.42: Correlation graph Color vs Band 3 reflectance value**

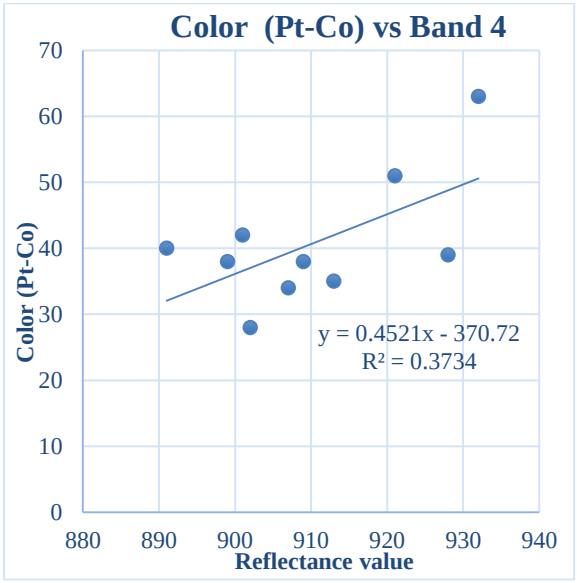

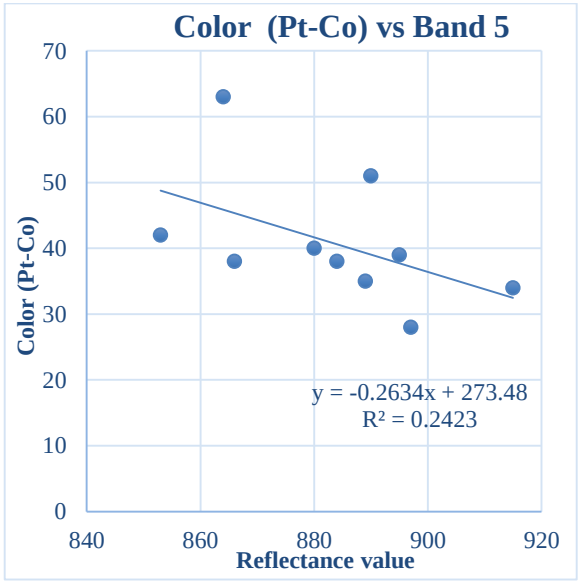

Fig 4.43: Correlation graph Color vs Band 4 reflectance value **Fig 4.44: Correlation graph Color vs Band 5 reflectance value**

The generated equations and corresponding regression values are given in Table 4.13:

Table 4.13: Generated equations and regression values-1 (Color)

Graph No. and Name	Generated Equation	Regression
Fig 4.49 - Color vs Band 2	y = 0.5832x - 796.15	R^2 = 0.478
Fig 4.50 - Color vs Band 3	y = 0.2693x - 267.85	R^2 = 0.1249
Fig 4.51 - Color vs Band 4	y = 0.4521x - 370.72	R^2 = 0.3734
Fig 4.52 - Color vs Band 5	y = -0.2634x + 273.48	R^2 = 0.2423

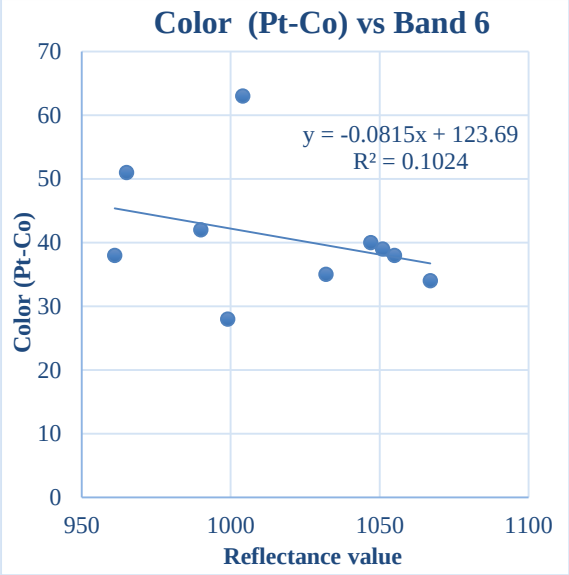

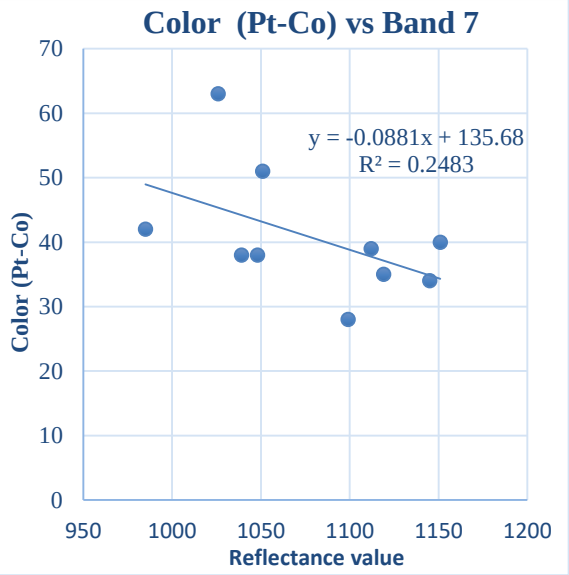

Fig 4.45: Correlation graph Color vs Band 6 reflectance value **Fig 4.46: Correlation graph Color vs Band 7 reflectance value**

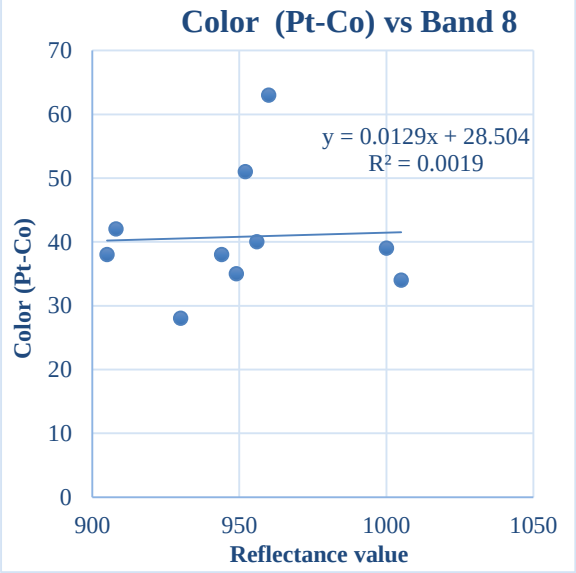

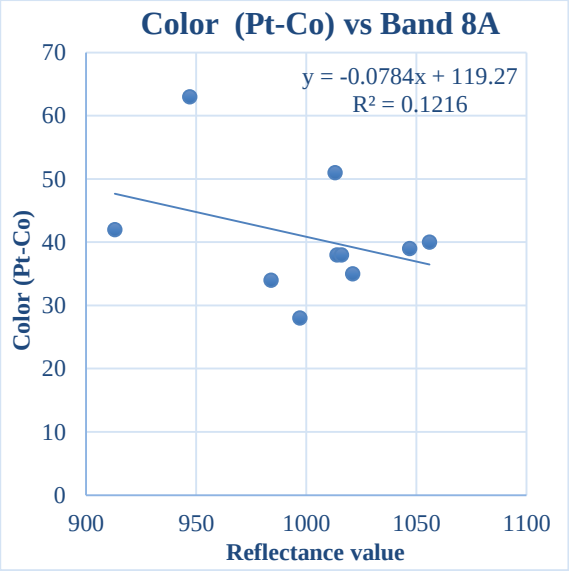

Fig 4.47: Correlation graph Color vs Band 8 reflectance value **Fig 4.48: Correlation graph Color vs Band 8A reflectance value**

The generated equations and corresponding regression values are given in Table 4.14:

Table 4.14: Generated equations and regression values-2 (Color)

Graph No. and Name	Generated Equation	Regression
Fig 4.53 - Color vs Band 6	y = -0.0815x + 123.69	R^2 = 0.1024
Fig 4.54 - Color vs Band 7	y = -0.0881x + 135.68	R^2 = 0.2483
Fig 4.55 - Color vs Band 8	y = 0.0129x + 28.504	R^2 = 0.0019
Fig 4.56 - Color vs Band 8A	y = -0.0784x + 119.27	R^2 = 0.1216

4.3.8 Results Summary

From all the plotted graphs, all the best generated equations are presented in Table 4.15

Table 4.15: Best regression equations for each parameter

Parameters	Regression equation	R^2	R
pH	y = -0.0017x + 8.652	0.3223	0.56771
DO	y = -0.0119x + 14.106	0.4857	0.6969
TDS	y = 0.3882x + 2.4325	0.2972	0.545119
TSS	y = 0.069x - 84.679	0.13	0.360546
Turbidity	y = 0.0646x - 53.251	0.4611	0.679038
Color	y = 0.5832x - 796.15	0.478	0.691386

4.4 Calculation of Water Indices

For the calculation of water indices Green, NIR, Red, SWIR1, and SWIR2 band values are needed. In Sentinel image classification Band 3 is classified as Green, Band 8 as NIR, Band 4 as Red, Band 11 as SWIR1 and Band 12 as SWIR2. The bands values and calculated water indices values are given in Table 4.16 and 4.17 respectively

Table 4.16: Reflectance value required for water index calculation

Location	Green	NIR	Red	SWIR1	SWIR2
1	1142	930	902	503	324
2	1166	960	932	463	249
3	1124	908	901	455	251
4	1133	905	899	467	280
5	1149	952	921	446	237
6	1147	944	909	450	235
7	1148	949	913	432	242
8	1153	1000	928	437	246
9	1163	1005	907	447	284
10	1138	956	891	441	250

.

Table 4.17: Calculated water index values

Location	MNDWI	AWEI	WRI	NDWI	NDMI
1	0.557981	1656.25	1.629984	0.102317	-0.01528
2	0.648057	2154.75	1.735318	0.096896	-0.0148
3	0.634909	2013.75	1.747196	0.106299	-0.00387
4	0.60368	1901.5	1.714768	0.111874	-0.00333
5	0.658009	2183.5	1.740959	0.093765	-0.01655
6	0.659913	2174.5	1.743851	0.097083	-0.01889
7	0.651799	2198.75	1.730479	0.094897	-0.01933
8	0.64832	2176.25	1.670144	0.071064	-0.03734
9	0.607464	2035.5	1.605896	0.072878	-0.05126
10	0.639769	2100.25	1.682421	0.086915	-0.03519

4.5 Regression Results for Water indices

Multiple Regression analysis was done between the quality parameter of different locations and the water indices. The regression values found from different combinations are given in Appendix A-1.

Detail equations for all the parameters with combination of different indices are presented in appendix A-2, A-3, A-4, A-5, A-6 and A-7 respectively.

From the equations the best proposed equations are shown in Table 4.18.

Table 4.18: Final selected regression models for each parameter

Parameters	Model	R
pH	-9.87645-23.8197MNDWI-0.00122AWEI+22.01719WRI-37.7915NDWI-20.6217NDMI	0.870979
TDS	10106.09+15798.6MNDWI+0.161611AWEI-12741.9WRI+20881.22NDWI+12729.76NDMI	0.940625
TSS	-248.253-368.898MNDWI-0.03074AWEI+378.8156WRI-967.321NDWI-234.24NDMI	0.951654
DO	-30.344+40.41507MNDWI-0.01572AWEI+25.81286WRI-57.2826NDWI-32.2898NDMI	0.852455
BOD	10.77553+5.320495MNDWI-0.00055AWEI-5.63421WRI+9.562542NDWI+4.713963NDMI	0.910899
Color	-1223.14-1917.88MNDWI+0.043892AWEI+1504.932WRI-2229.94NDWI-1549.58NDMI	0.667838
Turbidity	-302.194-537.596MNDWI-0.00109AWEI+420.5052WRI-792.054NDWI-383.5NDMI	0.845773

4.6 Results from Equations Developed with Reflectance Values

As stated earlier, water was collected along the mid-section of the river. All the water parameters were well within the allowable limit. But the scenario is not same near the tannery side of river. The water was constantly getting mixed with the tannery effluent. As both the upstream and downstream portion of the river have been covered, the overall condition of the river water flowing through the tannery side was taken in our study part. From the simple linear graphs, the correlation values were very moderate for pH. Regression values were in the range of 0.005-0.568. Like pH, the regression values for TDS was also close to 0.6. As all the linear equations were developed with the reflectance values only, the time maintenance for the sample collection was very crucial. But it could not be overcome due to the lacking of boating facility. So all the regression values were low to moderate for each water parameter.

The correlation value for TSS was found very low. The highest value was 0.3. This result means that none of the bands gave good results for this particular parameter. However, for further study, multiple images may be analyzed to generate a suitable equation for this parameter.

The best regression values obtained in this particular study were for DO, Turbidity and Color. The values are 0.69, 0.68 and 0.69 respectively. If more number of band values from different days could be incorporated, the results would have been more accurate. For the first time linear approaches with only the reflectance values have been done in this study. It can be very useful to use in a water body where the stations are fixed and time interval to go to one point from another will be very less. The tannery side length is not that much in Dhaleshwari River. So, monthly sample collection and subsequently satellite image processing for the same days can produce more equations with stronger regression values which can help to establish a better monitoring system.

4.7 Results from Equations Developed with Indices Values

Numerous important water indices have been calculated with the reflectance values from selected bands. Detail description and the formulas of water indices are described in methodology chapter. Equations with different combinations of water indices have been developed and regression values were analyzed. It can be seen that regression values range from 0.7-0.9 which is much better than the previous types of equations. Total 5 important water indices were used in this research. At first simple equations with a single index were developed for each parameter. All the regression values are shown in Table 10.1. A total of 20 equations have been developed for pH. The regression values vary from 0.75 to 0.87, which means each of the models represents very good regression. For TDS, a total of 23 equations have been developed. Highest regression value is 0.95, which incorporates all the water indices in the equation. This same procedure has been followed for rest of the parameters. The result shows that for TSS, Color, Turbidity, DO the regression values are also very high. So it can be said that, for this particular portion of Dhaleshwari River, important water indices are much effective in monitoring the water quality. But to use the linear equations with only reflectance values, more images should be used to establish more effective equations.

4.8 Validation

To validate the established models, an image sample of 18 December, 2018 was downloaded and analyzed. The reflectance values were extracted and water indices were calculated. Then the index values were applied in the models to calculate the water quality parameter of selected locations. The result from the derived equations and percentage error between field data and measured data are shown in Table 4.19:

Table 4.19: Model derived water quality parameters and error percentage.

Location	Values/Error	pH	TDS	TSS	DO	Color	Turbidity
1.	From Model	7.16	420	14	2.98	79	6.98
	From Lab Test	(7.23)	(427)	(14.2)	(3.03)	(77.5)	(7.12)
	% of Error	(0.96%)	(1.64%)	(1.41%)	(1.65%)	(1.94%)	(1.97%)
2.	From Model	7.15	417.2	13	2.6	66	5.90
	From Lab Test	(7.28)	(425)	(13.1)	(2.65)	(65)	(6.01)
	% of Error	(1.79%)	(1.84%)	(0.76%)	(1.89%)	(1.54%)	(1.83%)
3.	From Model	6.93	425	12.7	3.2	47	4.7
	From Lab Test	(6.85)	(431)	(13)	(3.15)	(48)	(4.76)
	% of Error	(1.17%)	(1.39%)	(2.3%)	(1.59%)	(2.08%)	(1.26%)
4.	From Model	7.01	437	12.1	2.81	37	7.2
	From Lab Test	(6.96)	(445)	(12)	(2.78)	(37.5)	(7.3)
	% of Error	(0.72%)	(1.8%)	(0.83%)	(1.08%)	(1.33%)	(1.37%)
5.	From Model	6.77	445	16	2.56	29	6.85
	From Lab Test	(6.89)	(454)	(16.2)	(2.52)	(29.5)	(6.96)
	% of Error	(1.74%)	(1.98%)	(1.23%)	(1.59%)	(1.69%)	(1.58%)

CHAPTER 5

CONCLUSION AND RECOMMENDATION

5.1 Conclusion

Monitoring the Dhaleshwari River water quality has become an important issue for the people living near the tannery area. Integrated Central Effluent Treatment Plant (CETP) is not totally functional yet. Moreover, there was a plan to incorporate a power plant in the plan to utilize the sludge produced in the area. But the plant is not established yet. As a result, the designed place for the plant has now become a dumping place of the sludge produced from the tanneries. So river water is being polluted day by day by these metals and stored sludge. The tannery area is also far away from the Dhaka. So it is very difficult to monitor the quality of river by lab testing in regular interval. Also there are a few numbers of boats available in that river. So it is not possible to test the desired sample all the time. So to have a continuous water monitoring, remote sensing may be a potential tool. The major findings from this research are below:

- ✓ The highest correlation value (R) for pH is 0.870979 with the equations developed from indices values. Using only the reflectance values the regression value was 0.56771.
- ✓ The highest correlation value (R) for TDS is 0.940625 with the equations developed from indices values. Using only the reflectance values the regression value was 0.545119.
- ✓ The highest correlation value (R) for TSS is 0.951654 with the equations developed from indices values. Using only the reflectance values the regression value was 0.36056.

- ✓ The highest correlation value (R) for DO is 0.852455 with the equations developed from indices values. Using only the reflectance values the regression value was 0.6969.
- ✓ The highest correlation value (R) for BOD is 0.910899 with the equations developed from indices values. Using only the reflectance values the regression value was 0.55826.
- ✓ The highest correlation value (R) for Color is 0.667838 with the equations developed from indices values. Using only the reflectance values the regression value was 0.691386.
- ✓ The highest correlation value (R) for Turbidity is 0.845773 with the equations developed from indices values. Using only the reflectance values the regression value was 0.679038.

The results show that, the equations with high regression models are generated for these parameters. These models can also be applied to measure the parameters of other water bodies as well.

5.2 Limitations of the Study

The high cloud cover values of the satellite images affect the correlation values of equations developed between field test values and values from water indices. So it was very difficult to obtain the images without zero cloud cover values. Generally, the satellite images pass Bangladesh between 11 AM to 12 AM. So it is better to collect samples between these times. But due to the lack of speed boats and motor boats the time maintenance could not be done. Approximate 30 minutes were needed to reach one point to another. Also ample amount of maps were not available. The main limitations for this study are:

- Sufficient digital maps were not available for the study. To get a correlation value closer to 1, a large number of clear images are needed for this research. Though

various days were selected for the study, due to the bad weather cloud cover value of the collected images were too high.

- The data collection time for both the days was between 11 AM to 2 AM. But satellite bands pass through Bangladesh around 11 AM to 12 AM.
- Due to the lack of motorized boat, the sample collection time interval between two consecutive points was too long. That also affected the results.

5.3 Recommendations

1. As the total tannery area is being shifted to Savar, the number of tanneries is increasing day by day. So the effluent from the tanneries will be increased. As the CETP is not fully functional yet, the treatment of the effluent is a prime concern. Already the aquatic plants have started to die. Both the physical and chemical characteristics of water have been affected severely. High organic loads and changes of water color are causing the death of aquatic plants. Some of the birds and wild lives have left the area already. The farmers used to utilize the river water for farming and other activities. But the pollution of the water has made it limited. There are 3-4 more outlets connected directly to the river. Discharges from this outlet are directly getting mixed with water. So proper functioning of CETP is mandatory to prevent further pollution of river.
2. It is mentioned earlier that there was a plan to incorporate a power plant to utilize the sludge produced in the treatment process. But as it is not setup yet, the area has become a dumping place. In the rainy season the sludge gets mixed with the river water. So it is high time to have a better plan of solid waste management there.
3. This study covered the total tannery side length of Dhaleshwari River. But it is necessary to know the extent of the downstream up to which the effluent is affecting the water.

4. In this study, samples from approx. mid reach of the river were taken for the analysis. But two or more sections may be taken for further study to have a précised result. Also more stations may be selected to have more data.
5. As it is mentioned earlier that satellite passing time on our country is between 11 AM to 12 PM. So some motor boats will be helpful to collect the water sample within this time. That will give better regression values.
6. Our laboratory was far away from the sample collection points. Otherwise we could have tested BOD and DO within a short time which could give us a better result.
7. This study was conducted with Sentinel 2A images. The images were available in the USGS website. There were some cloud cover values. In the further study, high resolution maps may be purchased and used in the analysis.
8. In most of the studies LANDSAT images were used for these types of research works. The resolution of Sentinel 2A and LANDSAT are different. As the images are not that much available. So equations for both the images may be established.
9. Finally, a detail mapping may be done to predict these seven water parameters at any point along the stream from the satellite images directly.
10. Digital map of a single day is considered here. For further study, bi-seasonal variation may be analyzed and incorporated in further study.
11. Basically this research was conducted at the end of the year 2018. The CETP was not fully functional at that time. So the effluent was not being fully treated before being discharged into the water. In the future when the ETP will be fully functional, better quality effluent is expected from the CETP. In that case the reflectance values from the surface water will be different. So regular monitoring will be needed immediately after the proper functioning of the treatment plant. On an average 5 to 6 images per month may be purchased and reflectance values may be used to produce equations for

a particular month. Subsequently these equations can be useful in determining the water quality parameters after the CETP operation.

12. The correlation values for color from both types of equations were low. In any further study, other bands of Sentinel 2A may be used. There are some other images like Landsat, Terra etc. Those satellite images may be used also to establish more precise equations for color.

References

[1] Usali, N., and Ismail, M. H. 2000, "Use of remote sensing and GIS in monitoring water quality". *Journal of Sustainable Development*, vol. 5, pp. 228.

[2] Panda, S.S., V. Garg, and I. Chaubey, 2004, "Artificial neural network application in lake water quality estimation using satellite imagery". *Journal of Environmental Informatics*, vol. 4, pp. 65-74.

[3] Al-bahrani, H. S. 2014, "Spatial prediction and classification of water quality parameters for irrigation use in the Euphrates River (Iraq) using GIS and satellite image analyses", *International Journal of Sustainable Development and Planning*, vol. 9, no.3, pp. 389-399.

[4] Abdullah, H. S. 2015, "Water quality assessment for Dokan Lake using Landsat 8 oli satellite images", *Phd thesis*, University of Sulaimani.

[5] Alparslan, E., Aydöner, C., Tufekci, V., and Tüfekci, H. 2007, "Water quality assessment at Omerli Dam using remote sensing techniques", *Environmental Monitoring And Assessment*, vol. 135(1-3), pp 391.

[6] Zanter, K. 2005, "landsat 8 (l8) data users handbook". *LSDS-1574* ,Version, 1.

[7] Mcfeeters, S.K., 1996, "The use of normalized difference water index (NDWI) in the delineation of open water features", *International Journal of Remote Sensing*, vol. 17, pp 1425–1432.

[8] Zhang, K., Thapa, B., Ross, M., and Gann, D. 2016, “Remote sensing of seasonal changes and disturbances in mangrove forest: a case study from South Florida”. *Ecosphere*, vol 7(6).

[9] Feyisa, G. L., Meilby, H., Fensholt, R., and Proud, S. R. 2014, “Automated water extraction index: a new technique for surface water mapping using Landsat imagery”. *Remote Sensing of Environment*, vol.140, pp. 23-35.

[10] Mukherjee, N. R., and Samuel, C. 2016, “Assessment of the temporal variations of surface water bodies in and around Chennai using Landsat imagery”, *Indian Journal of Science and Technology*, vol. 9 pp.18.

[11] Mustafa, T. M., Hassoon, K. I., Hussain, M. H., and Modher, H, 2017, “Using water indices (NDWI, MNDWI, NDMI, WRI and AWEI) to detect physical and chemical parameters by apply remote sensing and GIS techniques”, *International Journal of Research, GRANTHAALAYAH*, vol 5(10).

[12] Dekker A. G., 1993, “Detection of optical water quality parameters for eutrophic waters by high resolution remote sensing”. *PhD Thesis*,Vrije Universiteit,Amsterdam.

[13] Ruddick K. G., Ovidio F., and Rijkeboer M. 2000, “Atmospheric correction of SeaWiFS imagery for turbid coastal and inland waters”, *Journal of Applied Optics*, vol. 39, no. 6, pp. 897–912.

[14] Sathyendranath S., Prieur L., and Morel A. 1987, “An evaluation of the problems of chlorophyll retrieval from ocean colour, for case 2 waters”. *Advances in Space Research*, vol. 7, no. 2, pp. 27–30.

[15] Yang W., Matsushita B., Chen J., and Fukushima T. 2011, “Estimating constituent concentrations in case ii waters from meris satellite data by semi-analytical model optimizing and look up tables”, *Remote Sensing of Environment*, vol. 115, no. 5, pp. 1247–1259.

[16] JaelanI L. M., Matsushita B., Yang W., and Fukushima T. 2013, “Evaluation of four meris atmospheric correction algorithms in Lake Kasumigaura, Japan”, *International Journal of Remote Sensing*, vol. 34, no. 24, pp. 8967–8985.

[17] JaelanI L. M., Matsushita B., Yang W., and Fukushima T. 2015, “An improved atmospheric correction algorithm for applying meris data to very turbid inland waters”, *International Journal of Applied Earth Observation and Geoinformation*, vol. 39, pp. 128–141.

[18] Sathyendranath S., Prieur L. and Morel A. 1987, "An evaluation of the problems of chlorophyll retrieval from ocean color, for case 2 waters," *Advances in Space Research*, vol. 7, no. 2, pp. 27–30.

[19] Yang W., Matsushita B., Chen J. and Fukushima T. 2011, "Estimating Constituent Concentrations in Case Ii Waters from MERIS Satellite Data by Semi-Analytical Model Optimizing and LookUp Tables," *Remote Sensing of Environment*, vol. 115, no. 5, pp. 1247–1259, 2011.

[20] Laili N., Arafah F., Jaelani L. M., Subehi L., Pamungkas A.,. Koenhardono E. S and Sulisetyono A. 2015,"Development of water quality parameter retrieval algorithms for estimating total suspended solids and chlorophyll-a concentration using landsat-8 imagery," *Joint International Geoinformation Conference on Remote Sensing*, Malaysia.

[21] Mobley C. D. 1999, "Estimation of the remote-sensing reflectance from above-surface measurements," *Applied Optics*, vol. 38, no. 36, pp. 7442-7455.

[22] Han L. and Jordan K. J. 2005, "Estimating and mapping chlorophyll-a concentration in Pensacola bay, Florida using landsat etm+ data," *International Journal of Remote Sensing*, vol. 26, no. 23, pp. 5245–5254.

[23] Abbasi, T. and Abbasi, S.A. 2012, "Water quality indices". *Elsevier, Amsterdam*, The Netherlands.

[24] Akbar, T. A., Hassan, Q. K. and Achari, G., 2014. "Development of remote sensing based models for surface water quality", *Clean – Soil, Air, Water*, vol. 42(8), pp. 1044–1051.

[25] Al-Bahrani and Razzaq A. 2012. “A satellite image model for prediction water quality index of Euphrates river in Iraq, Baghdad” .*Phd Thesis*, University of Baghdad.

[26] Ali, S. S. & Salley, S. K. R., 2003. “Numerical groundwater flow modeling for the intwrgranular aquifer in sarsian sub-basin, Dokan lake, Iraqi kurdistan region”. *Journal of Zankoy Sulaimani-Part A,* vol. 15(1), pp. 125-141.

[27] Almdny, A. H., Belhaj, O. and Afan, A. M., 2010. “Impact of water quality on the spatial distribution of vegetation covers in the coastal regions with remote sensing and GIS methods”. *Fourteenth International Water Technology Conference IWTC 14*, Cairo, Egypt.

[28] Almdny, A. H., Ekhmaj, A. I., Abdul Aziz, A. M. & AL Jaml, H., 2008. “Possibility of using GIS and remote sensing approach in monitoring of change in plant cover due to change in water quality in coastal regions”. *Twelfth International Water Technology Conference, IWTC12*. Alexandria, Egypt,

[29] Alparslan, E., Aydöner, C., Tufekci, V. & Tüfekci, H., 2007, “Water quality assessment at Omerli Dam using remote sensing techniques”. *Environmental Monitoring Assessment*, vol. 135, pp. 391-398.

[30] Alparslan, E., Gonca Coşkun, H. & Alg, U., 2010. “An Investigation on Water Quality of Darlik Dam Drinking Water using Satellite Images”, vol. 10, pp.1293– 1306.

Appendix- A

Table A-1: Summary of Regression Values from Different Indices

Parameter	pH	TDS	TSS	DO	COLOR	Turbidity
MNDWI, AWEI	0.794458	0.704787	0.33802	0.814088	0.571837	0.258441
MNDWI, NDWI	0.730738	0.686405	0.554094	0.533223	0.600928	0.38058
MNDWI, NDMI	0.794159	0.782264	0.404257	0.576427	0.618401	0.232247
MNDWI, WRI	0.770226	0.746627	0.465258	0.557385	0.613375	0.283962
AWEI, WRI	0.799176	0.745477	0.474898	0.662037	0.622786	0.283941
AWEI, NDWI	0.762502	0.704305	0.623505	0.587288	0.608204	0.396555
MNDWI	0.5768	0.547539	0.33749	0.30887	0.56143	0.2027
NDWI	0.56648	0.52621	0.35270	0.49285	0.08307	0.26851
NDMI	0.57236	0.58387	0.20639	0.50069	0.23259	0.10344
AWEI	0.69993	0.64475	0.32062	0.49558	0.513225	0.1536
WRI	0.02236	0.007071	0.464435	0.127279	0.56418	0.2837
AWEI, NDMI	0.809062	0.776318	0.438519	0.628239	0.637111	0.213434
WRI, NDMI	0.812503	0.810877	0.490562	0.584595	0.60443	0.311021
WRI, NDWI	0.692105	0.631764	0.479023	0.521577	0.625674	0.314211
NDMI, NDWI	0.577976	0.588428	0.517604	0.504528	0.471037	0.523282
MNDWI, AWEI, WRI	0.80374	0.749221	0.611255	0.846599	0.631145	0.283968
MNDWI, AWEI, NDWI	0.795174	0.712868	0.761381	0.851294	0.608356	0.408177
MNDWI, AWEI, WRI, NDWI	0.864587	0.91523	0.949008	0.851811	0.659292	0.820555
MNDWI, AWEI, WRI, NDWI, NDMI	0.870979	0.940625	0.951654	0.852455	0.667838	0.845773
MNDWI, AWEI, NDMI	0.813811	0.7824	0.488727	0.840704	0.641979	0.259959
MNDWI, WRI, NDMI	0.827956	0.858028	0.860212	0.593416	0.623062	0.698862
MNDWI, NDWI, NDMI	0.835159	0.888765	0.885446	0.586777	0.629655	0.778837
AWEI, NDWI, NDMI	0.853273	0.880277	0.922644	0.650671	0.645918	0.75942
AWEI, WRI, NDMI	0.813276	0.833513	0.546019	0.715616	0.646912	0.58364
AWEI, WRI, NDWI	0.848452	0.809941	0.916797	0.795577	0.625798	0.609055

Table A-2: Regression Equations from Water Indices- pH

Equation	R
6.538406+5.865029MNDWI-0.001605332AWEI	0.794458
7.728687-1.93862MNDWI+4.577815NDWI	0.730738
8.458391-2.25574MNDWI+4.72758NDMI	0.794159
6.572744-4.31875MNDWI+1.8148WRI	0.770226
6.430575-0.00071AWEI+1.160705WRI	0.799176
7.515085-0.00043AWEI+3.309047NDWI	0.762502
-0.0005AWEI + 8.0441	0.69993
7.950819-0.00046AWEI+3.633415NDMI	0.809062
10.65844-2.068WRI+9.71278NDMI	0.812503
8.261699-1.23342WRI+8.225441NDWI	0.692105
6.363049+2.633035MNDWI-0.00113AWEI+0.723021WRI	0.80374
6.600917+5.276987MNDWI-0.00148AWEI+0.553303NDWI	0.795174
2.434874-7.27444MNDWI-0.00101AWEI+7.663557WRI-19.8701NDWI	0.864587
-9.87645-23.8197MNDWI-0.00122AWEI+22.01719WRI-37.7915NDWI-20.6217NDMI	0.870979
7.397601+2.257918MNDWI-0.00089AWEI+2.603543NDMI	0.813811
15.04095+4.929096MNDWI--6.34401WRI+20.04704NDMI	0.827956
9.906697-2.93665MNDWI-9.18161NDWI+12.19186NDMI	0.835159
9.296656-0.00059AWEI-9.62173NDWI+11.12579NDMI	0.853273
9.865973-0.00014AWEI-1.45655WRI+7.90357NDMI	0.813276
3.799205-0.00162AWEI+4.491326WRI-12.5017NDWI	0.848452

Table A-3: Regression Equations from Water Indices- TDS

Equation	R
455.7043-1330.38MNDWI+0.390606AWEI	0.704787
-13.7213+638.8997MNDWI-1449.31NDMI	0.782264
548.2737+1254.329MNDWI-540.581WRI	0.746627
582.9931+0.199602AWEI-337.259WRI	0.745477
262.6235+0.118869AWEI-928.646NDWI	0.704305
143.928+0.122236AWEI-1159.5NDMI	0.776318
-669.457+604.3599WRI-2904.18NDMI	0.810877
565.3058+689.6819MNDWI+0.091524AWEI-451.903WRI	0.749221
396.3217-771.765MNDWI+0.272127AWEI-525.615NDWI	0.712868
2506.321+5585.225MNDWI+0.034921AWEI-3881.4WRI+9818.316NDWI	0.91523
10106.09+15798.6MNDWI+0.161611AWEI-12741.9WRI+20881.22NDWI+12729.76NDMI	0.940625
-39.8415+750.0413MNDWI-0.02192AWEI-1501.61NDMI	0.7824
-2982.01-2600.98MNDWI+2860.724WRI-8357.36NDMI	0.858028
-721.72+971.7586MNDWI+4488.394NDWI-5098.19NDMI	0.888765
-473.102+0.185784AWEI+4411.302NDWI-4594.55NDMI	0.880277
-1961.16-0.22643AWEI+1600.998WRI-5853.14NDMI	0.833513
1458.804+0.500742AWEI-1445.8WRI+4161.006NDWI	0.809941

Table A-4: Regression Equations from Water Indices- TSS

Equation	R
8.888768+172.4342MNDWI-0.0416AWEI-188.716NDWI	0.761381
-108.41-180.961MNDWI-0.02841AWEI+215.7737WRI-763.753NDWI	0.949008
-248.253-368.898MNDWI-0.03074AWEI+378.8156WRI-967.321NDWI-234.24NDMI	0.951654
388.9767+369.0437MNDWI-347.069WRI+805.5824NDMI	0.860212
103.3282-59.0367MNDWI-472.109NDWI+351.2901NDMI	0.885446
92.13325-0.01221AWEI-486.05NDWI+333.3079NDMI	0.922644
-74.47-0.0435AWEI+136.8602WRI-580.456NDWI	0.916797

Table A-5: Regression Equations from Water Indices- DO

Equation	R
-6.9559+50.18642MNDWI-0.01102AWEI	0.814088
-5.28994+80.89182MNDWI-0.01557AWEI-6.86903WRI	0.846599
-9.25227+71.78844MNDWI-0.0156AWEI-20.3259NDWI	0.851294
-11.0667+66.32187MNDWI-0.0154AWEI+3.33774WRI-29.2209NDWI	0.851811
-30.344+40.41507MNDWI-0.01572AWEI+25.81286WRI-57.2826NDWI-32.2898NDMI	0.852455
-12.0457+71.55477MNDWI-0.01526AWEI-15.4233NDMI	0.840704
-34.0416-0.00805AWEI+30.0623WRI-70.9194NDMI	0.715616

Table A-6: Regression Equations from Water Indices- Color

Equation	R
-91.5885+185.7465MNDWI+162.5743NDWI	0.600928
-65.6814+174.4629MNDWI+166.928NDMI	0.618401
-133.506+100.3032MNDWI+65.29941WRI	0.613375
-129.422+0.017519AWEI+78.90251WRI	0.622786
-62.156+0.037958AWEI+265.3336NDWI	0.608204
-26.187+0.035159AWEI+251.2083NDMI	0.637111
-216.103+148.6645WRI-192.671NDMI	0.60443
-179.909+142.9495WRI-238.972NDWI	0.625674
-66.2566+23.67008MNDWI+0.033257AWEI+252.9726NDWI	0.608356
-298.032-674.622MNDWI+0.059314AWEI+426.3578WRI-883.269NDWI	0.659292
-1223.14-1917.88MNDWI+0.043892AWEI+1504.932WRI-2229.94NDWI-1549.58NDMI	0.667838
10.76731-150.826MNDWI+0.064146AWEI+320.0026NDMI	0.641979
93.23882+347.9238MNDWI-153.161WRI+536.7802NDMI	0.623062
-16.3289+151.2603MNDWI-312.873NDWI+421.281NDMI	0.629655
13.03094+0.03112AWEI-280.379NDWI+469.5377NDMI	0.645918
166.918+0.067143AWEI-146.864WRI+681.768NDMI	0.646912
-171.506+0.003049AWEI+132.1694WRI-199.941NDWI	0.625798

Table A-7: Regression Equations from Water Indices- Turbidity

Equation	R
-73.2412-229.905MNDWI+0.002729AWEI+153.5722WRI-458.77NDWI	0.820555
-302.194-537.596MNDWI-0.00109AWEI+420.5052WRI-792.054NDWI-383.5NDMI	0.845773
187.5514+185.1343MNDWI-170.653WRI+402.7124NDMI	0.698862
50.28689-26.8507MNDWI-252.347NDWI+195.7692NDMI	0.778837
42.77766-0.00498AWEI-247.169NDWI+179.789NDMI	0.75942